



HAL
open science

**Structural investigation of new tellurite glasses
belonging to the TeO₂-NbO_{2.5}-WO₃ system, and a
study of their linear and nonlinear optical properties**

Mohammed Reda Zaki, David Hamani, Maggy Dutreilh-Colas, Jean-René Duclere, Jonathan de Clermont-Gallerande, Tomokatsu Hayakawa, Olivier Masson, Philippe Thomas

► **To cite this version:**

Mohammed Reda Zaki, David Hamani, Maggy Dutreilh-Colas, Jean-René Duclere, Jonathan de Clermont-Gallerande, et al.. Structural investigation of new tellurite glasses belonging to the TeO₂-NbO_{2.5}-WO₃ system, and a study of their linear and nonlinear optical properties. *Journal of Non-Crystalline Solids*, 2019, 512, pp.161-173. 10.1016/j.jnoncrysol.2019.02.027 . hal-02361653

HAL Id: hal-02361653

<https://unilim.hal.science/hal-02361653>

Submitted on 17 Feb 2020

HAL is a multi-disciplinary open access archive for the deposit and dissemination of scientific research documents, whether they are published or not. The documents may come from teaching and research institutions in France or abroad, or from public or private research centers.

L'archive ouverte pluridisciplinaire **HAL**, est destinée au dépôt et à la diffusion de documents scientifiques de niveau recherche, publiés ou non, émanant des établissements d'enseignement et de recherche français ou étrangers, des laboratoires publics ou privés.

Structural investigation of new tellurite glasses belonging to the TeO₂-NbO_{2.5}-WO₃ system, and a study of their linear and nonlinear optical properties

Mohammed Reda ZAKI¹, David HAMANI^{1*}, Maggy DUTREILH-COLAS¹, Jean-René DUCLÈRE¹, Jonathan DE CLERMONT-GALLERANDE¹, Tomokatsu HAYAKAWA², Olivier MASSON¹ and Philippe THOMAS¹

¹ Institut de Recherche sur les Céramiques (IRCER) – UMR CNRS 7315, Université de Limoges, Centre Européen de la Céramique, 12 rue Atlantis, 87068 Limoges Cedex, France

² Nagoya Institute of Technology (NITECH), Department of Life Science and Applied Chemistry, Field of Advanced Ceramics, Gokiso, Showa, Nagoya 466-8555, Japan

*** Corresponding author.**

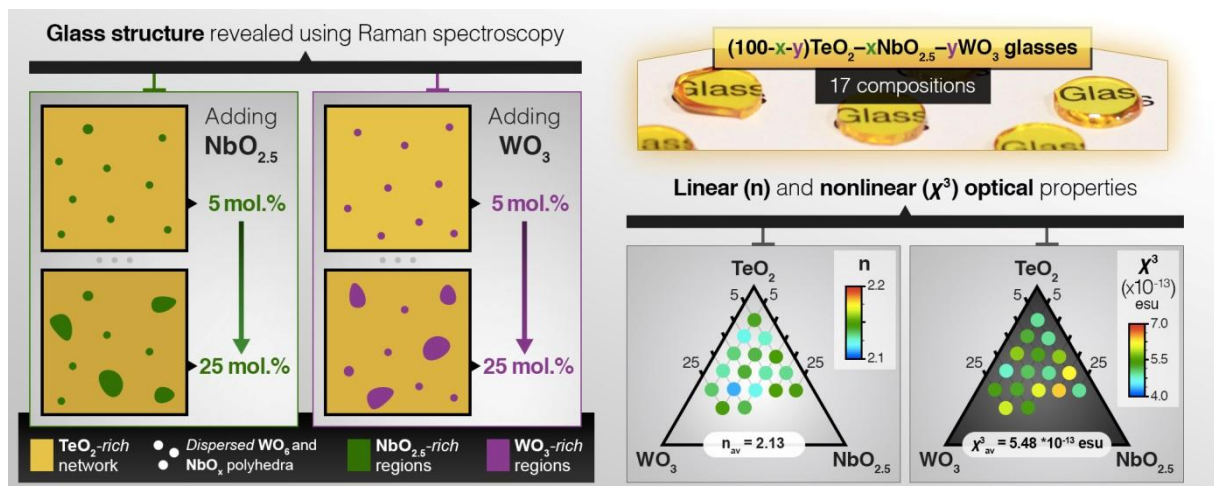
David Hamani, IRCER – UMR CNRS 7315, Centre Européen de la Céramique, 12 rue Atlantis, 87068 Limoges Cedex, FRANCE, david.hamani@unilim.fr, +33587502379

Abstract. (189 words)

The glass-forming domain, density, thermal, structural and optical properties of new glasses within the TeO₂-NbO_{2.5}-WO₃ system have been investigated. By means of Raman spectroscopy, a thorough structural analysis of these glasses has been undertaken on the basis of a full-scale spectral decomposition process. The optical transmission window, refractive index dispersion and third-order nonlinear susceptibilities $\chi^{(3)}$ were measured by UV-Vis-NIR spectroscopy, spectroscopic ellipsometry and Z-scan method respectively. Consistent correlations are successfully established between the measured structural, linear and nonlinear optical properties. In general, the structural features of the glass network are found to evolve mildly upon adding NbO_{2.5} or WO₃. Nonetheless, a weak structural depolymerization of the Te–O–Te bond network as a result of adding NbO_{2.5} is evidenced and discussed in detail.

Upon continuous addition of $\text{NbO}_{2.5}$ and/or WO_3 , the glass network becomes progressively richer in $\text{NbO}_{2.5}$ -rich and/or WO_3 -rich regions before the crystallization of $\text{Nb}_6\text{TeO}_{17}$ ($\text{NbO}_{2.5}:\text{TeO}_2$ ratio of 6:1) and $\text{WO}_{2.83}$ compounds respectively. The studied glasses exhibit high linear refractive indices with an average of ~ 2.13 and very high third-order nonlinear susceptibilities $\chi^{(3)}$ with an average of 5.48×10^{-13} esu (~ 37 times higher than that of SiO_2 glass).

Graphical abstract.



Keywords.

Tellurite glasses; Glass structure; Raman spectroscopy; Optical linearity; Optical nonlinearity.

1. Introduction.

Tellurium oxide (TeO_2)-based glasses have been widely investigated as promising materials for specific optical applications, and this mostly due to their excellent nonlinear optical properties [1–4]. Furthermore, such specific applications of tellurite glasses are related to their interesting thermal properties (low glass transition temperatures) and their capacity to be drawn into classical core/clad optical fibers [5], or even specialty fibers dedicated for the generation of broad supercontinuum [6]. Other potential applications for tellurite bulk glasses and fibers, still in connection with the large third order optical nonlinearity, will be Raman amplification [7–9], ultra-fast optical switches or electro-optic modulators [10,11]. Finally, recent works also demonstrate the potentiality of rare-earth doped tellurites to be employed as laser fibers beyond $2 \mu\text{m}$ [12,13].

The structural origin of this large optical nonlinearity of TeO_2 -based glasses derives mainly from the existence of the Te^{4+} electronic lone pair [14–18] and characteristic Te–O–Te bridges [3,19–21]. According to the literature, adding transition-metal oxides, such as niobium oxide Nb_2O_5 or tungsten oxide WO_3 , may increase or at least maintain constant the linear and nonlinear optical indices of TeO_2 -based glasses [1]. Contrarily, it has been shown that adding modifier oxides, such as alkali oxides, curtails such properties [3,22]. This transformation is commonly referred to as ‘structural depolymerization’ of the TeO_2 -rich network since it diminishes the network crosslinking density via breaking the Te–O–Te bridges. From the short-range structural viewpoint, it corresponds to the transformation of TeO_4 disphenoids into TeO_3 trigonal pyramids *via* TeO_{3+1} distorted disphenoids [3,23,24].

A great deal of effort has been devoted to the study of the binary $(100-x)\text{TeO}_2-x\text{WO}_3$ glassy system uncovering its glass-forming domain with a WO_3 content ranging between 5 and 40 mol.% [1,25–30]. It has been demonstrated that incorporating WO_3 in the TeO_2 -rich glass

network progressively enhances both thermal and optical (linear and nonlinear) properties [1,27,31].

Several studies have been conducted on the binary $(100-x)\text{TeO}_2-x\text{NbO}_{2.5}$ glassy system uncovering its glass-forming domain with a maximal $\text{NbO}_{2.5}$ content of 33.4-40 mol.% according to different authors [1,30,32–37]. It has been shown that adding $\text{NbO}_{2.5}$ to the TeO_2 -rich glass network enhances both the linear and nonlinear optical properties [1] and increases the thermal stability [30,32] which is a crucial requirement in some optical glass manufacturing processes, *e.g.*, optical fiber drawing [38]. An improvement of the network reinforcement and mechanical strength was also reported [39]. The structural features of these glasses have been extensively investigated by various techniques: X-ray and neutron diffraction (see *e.g.*, [40]), X-ray absorption spectroscopy [41], IR and Raman [30,34,42] spectroscopies. It is accepted among the previous investigators that adding $\text{NbO}_{2.5}$ leads to a structural depolymerization [30,36,41]. According to Berthereau *et al.* [41], the predominant units in $(100-x)\text{TeO}_2-x\text{NbO}_{2.5}$ glasses ($x = 9.5, 18.2, 26.1, 33.4$ mol.%) are TeO_4 and TeO_{3+1} and the proportion of the latter increases upon adding $\text{NbO}_{2.5}$ as suggested from the extended X-ray absorption fine structure (EXAFS) results. Hoppe *et al.* [40] investigated the structure of $(100-x)\text{TeO}_2-x\text{NbO}_{2.5}$ ($x = 11.4, 18.2$ and 30.5 mol.%) glasses and argued that a structural transition from network-modifying ($x \leq 18.2$ mol.%) to network-forming behavior ($x > 18.2$ mol.%) takes place upon adding $\text{NbO}_{2.5}$ with the formation of Nb–O–Nb bridges. By means of Raman spectroscopy, Soulis *et al.* [34] argued that the bond networks of $(100-x)\text{TeO}_2-x\text{NbO}_{2.5}$ ($x = 9.5, 18.2, 26.1, 33.4$ and 40 mol.%) glasses contain three types of linkages, namely Te–O–Te, Te–O–Nb and Nb–O–Nb bridges. More recently, two more studies by Lin *et al.* [36] and Kaur *et al.* [30] agree with the previously described role of $\text{NbO}_{2.5}$ in reducing the connectivity of Te–O–Te bond network by transforming the TeO_4 into TeO_{3+1} and TeO_3 units.

This work is a part of an investigation on TeO₂-based glasses containing two transition-metal oxides. After dealing with the (100-x-y)TeO₂-xTiO₂-yWO₃ glassy system [43], we have embarked on investigating the (100-x-y)TeO₂-xNbO_{2.5}-yWO₃ system (labeled TN_xW_y). To the best of our knowledge, aside from few investigations on the specific compositions given below, there is no reported systematic study within this ternary glass system. Carreaud *et al.* [44] and Dai *et al.* [45] recorded the Raman spectra of 75TeO₂-20NbO_{2.5}-5WO₃ and 72TeO₂-18NbO_{2.5}-10WO₃ glass compositions respectively along with their thermal and linear optical properties; Muñoz-Martín [46] measured the linear and nonlinear optical properties of the 80TeO₂-5Nb₂O₅-15WO₃ glass composition. In addition, Er³⁺ and Yb³⁺ doped TeO₂-Nb₂O₅-WO₃ glass compositions have been investigated as potential candidate materials for broadband amplifiers [47,48]. A high linear optical response was measured from these glasses with refractive indices in the order of ~2.1.

The aim of the present paper is to report, for the first time, the glass-forming domain within the TN_xW_y system and the measured properties from the prepared glasses, namely, their thermal characteristics, structural features by means of Raman spectroscopy, linear optical properties using UV-Vis-NIR spectroscopy and spectroscopic ellipsometry, and nonlinear optical response from Z-scan measurements. The focus is laid on the evolution of these properties as a function of NbO_{2.5} and WO₃ contents.

2. Experimental details.

New glasses were prepared within the ternary TN_xW_y system by the conventional melting-quenching technique using α-TeO₂ (99.99%), Nb₂O₅ (99.99%) and WO₃ (99.8%) from Alfa Aesar. In appropriate proportions, the raw dried powders have been ground for 40 min using agate mortar and pestle, and melted in Pt crucibles at 850 °C for 1 h. Under these

experimental conditions, seventeen glass samples in the form of pellets were prepared from batches weighing 2 g, stirred three times during melting and quenched into a brass ring put over a preheated brass block at 150 °C. After cooling down to room temperature from 150 °C, the pellets were systematically annealed at 15 °C below their glass transition temperatures for 12 h at heating/cooling rates of 2 °C/min in order to release the mechanical stresses resulting from the thermal quenching. Serving as a reference sample in the structural study of TN_xW_y glasses, we have prepared TeO₂ glass by the fast-quenching of a pure TeO₂ melt from 850 °C down to approximately -11 °C (using an ice bath containing NaCl and ethanol) after 1 h spent inside the furnace during which the melt was stirred three times.

The amorphous state of the samples was checked by means of powder X-ray diffraction using Bruker D8 Advance diffractometer with Bragg-Brentano geometry (Cu K_{α1} wavelength of 1.5406 Å, 2θ range of 10-70° with a step of 0.02° and 1 s per step). The glass samples were analyzed by energy dispersive X-ray microanalysis (EDS) using a Quanta FEG-450 scanning electron microscope. The elemental analysis results suggested a good agreement between the experimental and theoretical glass compositions. The characteristic glass transition (T_g) and onset crystallization (T_O) temperatures of the glass samples were measured by heat flux differential scanning calorimetry (DSC) using NETZSCH STA 449 F3 Jupiter equipment. The measurements were performed on glass fragments of about 25 ± 5 mg using Pt pans under N₂ atmosphere between room temperature and 720 °C at a heating rate of 10 °C/min. Densities of glass powder samples weighing 150 ± 20 mg were measured by helium pycnometry using Accupyc II 1340 Micromeritics pycnometer.

The Raman spectra were recorded at 514.5 nm and a laser power of 30 mW using T64000 Horiba Jobin-Yvon spectrophotometer operating in triple subtractive configuration (1800 grooves/mm) and equipped with a CCD detector. The objective lens x50LWD was used to record the spectra along the 15-1100 cm⁻¹ wavenumber range with a spectral resolution of 2.5

cm^{-1} and acquisition time of 10 s. Three spectra from each sample have been recorded from three different spots. No baseline correction treatments were performed on any of the measured spectra, and the as-recorded intensities of each spectrum were divided by its total area. Using Focus 1.0 program [49], the total-area averaged Raman spectra were decomposed in the entire wavenumber range ($15\text{-}1100\text{ cm}^{-1}$) using a log-normal distribution for the boson peak (labeled band A hereafter) and twelve Gaussian functions for the rest (labeled bands B–M). The recomposed spectra match well with the experimental ones, with chi-square reliability values less than 0.05.

The optical transmission of TNxWy glasses was evaluated by measuring the UV-Vis-NIR spectra from double side polished pellets of 1.44-1.47 mm in thickness in the 300-3300 nm range using the Varian Cary 5000 spectrophotometer. From the same samples, the refractive indices were recorded by spectroscopic ellipsometry using Horiba Jobin-Yvon UVISSEL ellipsometer with a fixed 60° incidence angle.

The third-order nonlinear susceptibilities $\chi^{(3)}$ were measured from TNxWy double-side polished glasses employing the Z-scan technique, and using a comparative route in respect with the data collected for a reference fused silica plate [50]. Pulses from regenerative Ti:sapphire laser (Spectra Physics, Hurricane) at 800 nm were used at a repetition rate of 1 kHz and with ~ 90 fs pulse duration. A lens ($f = 200$ mm) was positioned along the optical path (Z axis), and the glass samples were moved forward and backward from the focal point ($Z = 0$ mm), namely along the Z range between -25 mm and +25 mm at intervals of 0.5 mm. At each step, the optical transmittance was measured with the optical power meter system (Newport 2930-C/818-SL silicon photodiodes in the close and open configurations [51]). The Z-scan measurement from each glass sample was repeated three times. Each consists in four measurements: two at 250 nW and two at 2 nW. The measured $\chi_{(\text{SiO}_2)}^{(3)}$ value from pure SiO_2 glass ($\approx 0.15 \cdot 10^{-13}$ esu at 800 nm reported by Milam [52]) was considered in order to extract

the $\chi^{(3)}$ values for TNxWy glasses. For a reliable comparison with other TeO₂-based glasses in the literature, we had to adjust the state-of-the-art values (those extracted by considering a $\chi_{(SiO_2)}^{(3)}$ value of $0.28 \cdot 10^{-13}$ esu at 1.9 μm reported by Kim *et al.* [53]) by dividing them by 1.87 which is the factor between the $\chi_{(SiO_2)}^{(3)}$ values reported by Kim *et al.* [53] and Milam [52] respectively. Such argumentation is developed in detail in [50]. Applying this factor to the pure TeO₂ glass leads to an adjusted $\chi^{(3)}$ value of $7.54 \cdot 10^{-13}$ esu based on the reported value of $14.10 \cdot 10^{-13}$ esu [53]. We have obtained the real part of the third-order nonlinear susceptibility $\text{Re}(\chi_{(glass)}^{(3)})$ from TNxWy glasses; more details can be found in the literature (*e.g.*, [54]) and lead to the following expression:

$$\text{Re}(\chi_{(glass)}^{(3)}) = \text{Re}(\chi_{(SiO_2)}^{(3)}) * \left(\frac{\Delta\phi_{(glass)}}{\Delta\phi_{(SiO_2)}} \cdot \frac{I_0_{(SiO_2)}}{I_0_{(glass)}} \cdot \frac{L_{eff}(SiO_2)}{L_{eff}(glass)} \cdot \frac{n_{(glass)}^2}{n_{(SiO_2)}^2} \right)$$

With $\Delta\phi$ corresponding to self-phase modulation which is proportional to the difference ΔT_{p-v} ($\Delta T_{p-v} \approx 0.406 \Delta\phi$ for small apertures [51]) between the maximum T_p (p for peak) transmittance and the minimum T_v (v for valley) transmittance. I_0 represents the intensity of the incident laser beam, L_{eff} the effective thickness of the sample and n the linear refractive index measured by spectroscopic ellipsometry.

3. Results and discussion.

3.1. Glass-forming domain

The amorphous state of TNxWy samples was analyzed using X-ray powder diffraction in order to determine the glass-forming domain given in Fig. 1(a)). The longest compositional lines extend from $x = 5$ to 25 mol.% in NbO_{2.5} and from $y = 5$ to 25 mol.% in WO₃. In total, seventeen melt compositions have yielded transparent yellowish glasses that shifted to honey-

brown with increasing WO_3 molar content and remained practically unchanged upon adding $\text{NbO}_{2.5}$ (*cf.* Fig. 1(b)). In partially crystallized TN_xW_30 samples, we detected the presence of $\text{WO}_{2.83}$ (or W_6O_{17}) crystals [55]. At relatively high $\text{NbO}_{2.5}$ content, crystals of $\text{Nb}_6\text{TeO}_{17}$ [56] are detected in TN15W25 , TN20W15 , TN25W10 and TN30W5 samples.

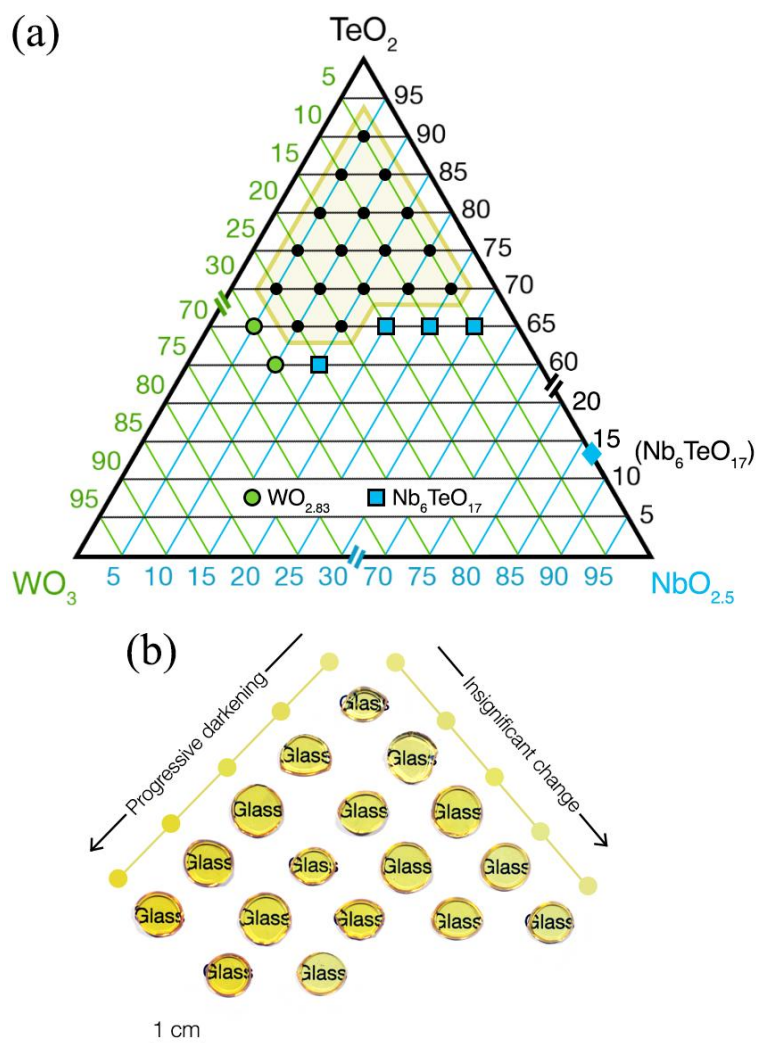


Fig. 1. (a) Glass-forming domain obtained in the $(100-x-y)\text{TeO}_2-x\text{NbO}_{2.5}-y\text{WO}_3$ system (labeled TN_xW_y) surrounded by the yellow frame. Blue and green colored squares and spots correspond to partially crystallized samples in $\text{WO}_{2.83}$ and $\text{Nb}_6\text{TeO}_{17}$ respectively. (b) Photograph of the obtained glass pellets in their polished state.

3.2. Density and thermal properties

In general, the measured densities ($\rho_{\min} = 4.51 \text{ g.cm}^{-3}$ and $\rho_{\max} = 5.15 \text{ g.cm}^{-3}$) increase with the addition of WO_3 and slightly decrease with larger amounts of $\text{NbO}_{2.5}$ (*cf.* Table 1). The density increase extent upon adding WO_3 at constant $\text{NbO}_{2.5}$ content varies from one series of samples to the other. For instance, an increase by $\sim 10\%$ is recorded from TN5W5 (4.67 g.cm^{-3}) to TN5W25 (5.15 g.cm^{-3}) and by $\sim 4\%$ from TN10W5 (4.87 g.cm^{-3}) to TN10W25 (5.06 g.cm^{-3}). On the other hand, the density's compositional dependence upon adding $\text{NbO}_{2.5}$ shows a peculiar behavior in TeO_2 -rich compositions as it first increases for instance by $\sim 4\%$ from TN5W5 (4.67 g.cm^{-3}) to TN10W5 (4.87 g.cm^{-3}) before decreasing by $\sim 7\%$ to TN25W5 (4.51 g.cm^{-3}). This unexpected behavior in the TeO_2 -richest compositions could be explained by their positions at the boundary of the glass-forming domain. In general, it can be argued that the compositional dependence of density follows the *additive density rule*: densities of raw oxides $\text{NbO}_{2.5}$, TeO_2 and WO_3 are respectively 4.55, 6.13 and 7.16 g.cm^{-3} . Thus, we assign the glass density increase upon adding WO_3 to the higher molar mass of WO_3 (231.8 g.mol^{-1}) compared to that of TeO_2 (159.6 g.mol^{-1}); and the decrease upon adding $\text{NbO}_{2.5}$ from 10 to 25 mol.% to its lower molar mass of 132.9 g.mol^{-1} .

The thermal properties of TN_xW_y glasses were measured to evaluate the compositional dependence of their glass transition temperatures T_g and thermal stabilities ΔT (*cf.* Table 1 for TN_xW_y glasses and Fig. 2 for TN_xW_5 glasses). The T_g increases linearly upon adding either $\text{NbO}_{2.5}$ or WO_3 ($T_{g(\min)} = 333 \text{ }^\circ\text{C}$ and $T_{g(\max)} = 403 \text{ }^\circ\text{C}$). It increases by $\sim 21\%$ from TN5W5 ($333 \text{ }^\circ\text{C}$) to TN25W5 ($403 \text{ }^\circ\text{C}$) and by $\sim 15\%$ from TN5W5 to TN5W25 ($381 \text{ }^\circ\text{C}$). We could assign the T_g increase predominantly to the fact that W–O and Nb–O bonds have higher dissociation energies compared to Te–O bonds, namely, 720, 726.5 and 377 kJ.mol^{-1} respectively [57].

It is worth pointing out that the thermal stabilities ($\Delta T = T_O - T_g$) of TN_xW_y glasses which reflect the ability of the glass network to resist against devitrification upon heating above T_g ,

are fairly moderate ($\Delta T_{\min}= 45$ °C and $\Delta T_{\max}= 70$ °C) with an average of ~ 60 °C. It appears that adding NbO_{2.5} or WO₃ does not significantly impact on ΔT from one TN_xW_y composition to another. By comparison, the thermal stabilities of TN_xW₅ samples are relatively lower than those reported for binary TeO₂-NbO_{2.5} glasses with values ranging between ~ 43 and ~ 98 °C according to Blanchandin *et al.* [33].

Sample	T _g (°C) ± 1	ΔT (°C) ± 1	Density (g/cm ³)	E _g (eV) ± 0.020	E _U (eV) ± 0.002	n _{1.5} [*] ± 0.010	n _∞ [§]	χ ⁽³⁾ (10 ⁻¹³ esu)
TN5W5	333	60	4.667 ± 0.007	2.920	0.114	2.116	2.142 ± 0.008	5.05 ± 1.00
TN10W5	348	49	4.870 ± 0.003	2.913	0.110	2.101	2.125 ± 0.005	4.99 ± 0.94
TN15W5	366	66	4.815 ± 0.004	2.904	0.107	2.102	2.149 ± 0.022	5.66 ± 1.33
TN20W5	382	70	4.723 ± 0.005	2.897	0.106	2.104	2.129 ± 0.019	6.24 ± 1.23
TN25W5	403	45	4.508 ± 0.014	2.892	0.105	2.098	2.145 ± 0.011	5.05 ± 1.61
TN5W10	346	61	4.777 ± 0.004	2.860	0.109	2.097	2.124 ± 0.006	5.33 ± 1.17
TN10W10	362	52	4.928 ± 0.006	2.855	0.107	2.090	2.134 ± 0.024	5.42 ± 1.16
TN15W10	378	67	4.871 ± 0.007	2.850	0.104	2.116	2.127 ± 0.019	5.03 ± 1.05
TN20W10	397	59	4.837 ± 0.006	2.847	0.104	2.064	2.149 ± 0.008	6.38 ± 2.11
TN5W15	360	69	4.993 ± 0.004	2.832	0.108	2.089	2.132 ± 0.006	5.62 ± 1.39
TN10W15	374	54	5.010 ± 0.014	2.827	0.107	2.057	2.140 ± 0.011	4.82 ± 1.11
TN15W15	387	60	4.962 ± 0.005	2.822	0.105	2.114	2.124 ± 0.008	6.05 ± 1.44
TN5W20	370	56	5.052 ± 0.002	2.802	0.108	2.107	2.128 ± 0.006	4.75 ± 0.95
TN10W20	386	65	5.061 ± 0.007	2.800	0.106	2.095	2.116 ± 0.008	5.27 ± 1.00
TN15W20	389	56	4.928 ± 0.002	2.796	0.107	2.107	2.138 ± 0.012	5.40 ± 1.22
TN5W25	381	55	5.153 ± 0.006	2.777	0.108	2.100	2.136 ± 0.023	5.36 ± 1.23
TN10W25	393	69	5.056 ± 0.006	2.775	0.106	2.095	2.145 ± 0.033	5.82 ± 1.05

Table 1. Thermal properties, densities, linear and nonlinear optical properties of TN_xW_y glasses.
 * Refractive indices obtained at $\lambda = 1.5 \mu\text{m}$ from transmission spectra. § Refractive indices derived from ellipsometric dispersion curves using Sellmeier's equation.

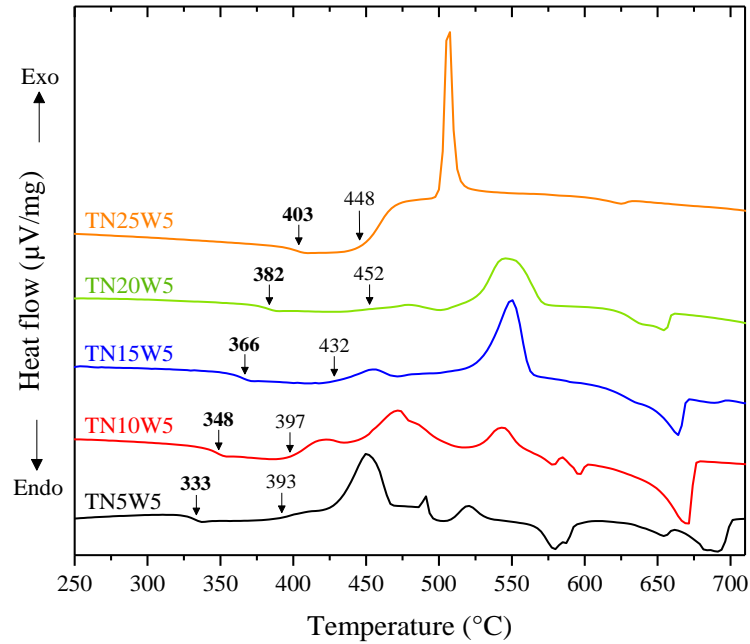


Fig. 2. DSC curves of TN_xW₅ glasses with the glass transition T_g and onset crystallization T_o temperatures given in bold and non-bold typefaces respectively.

The recorded sequence of exothermic peaks from the DSC curves of TN_xW₅ glasses (Fig. 2) is in relatively good agreement with the binary TeO₂-NbO_{2.5} glasses (*cf.* Fig. 3 in [33]); the exothermic peaks of the former are broader, probably due to a more disordered glass network, manifested by the presence of additional W–O coordination polyhedra. Therefore, the crystallizing phases from TN_xW₅ glasses can be assigned in agreement with those crystallizing from the binary glasses, *i.e.*, δ -, γ - and α -TeO₂ and then Nb₂Te₄O₁₃ depending on the NbO_{2.5} content.

3.3. Structural properties

The recorded spectra from TN_xW_y glasses are jointly presented in Fig. 3. Since the same structural evolutions are observed from TN_xW_y ($y = 5, 10, 15, 20$ and 25 mol.%) sets of samples, we suggest to focus on the set of TN_xW₅ to highlight the effect of adding NbO_{2.5} since it corresponds to the set with the lowest WO₃ influence.

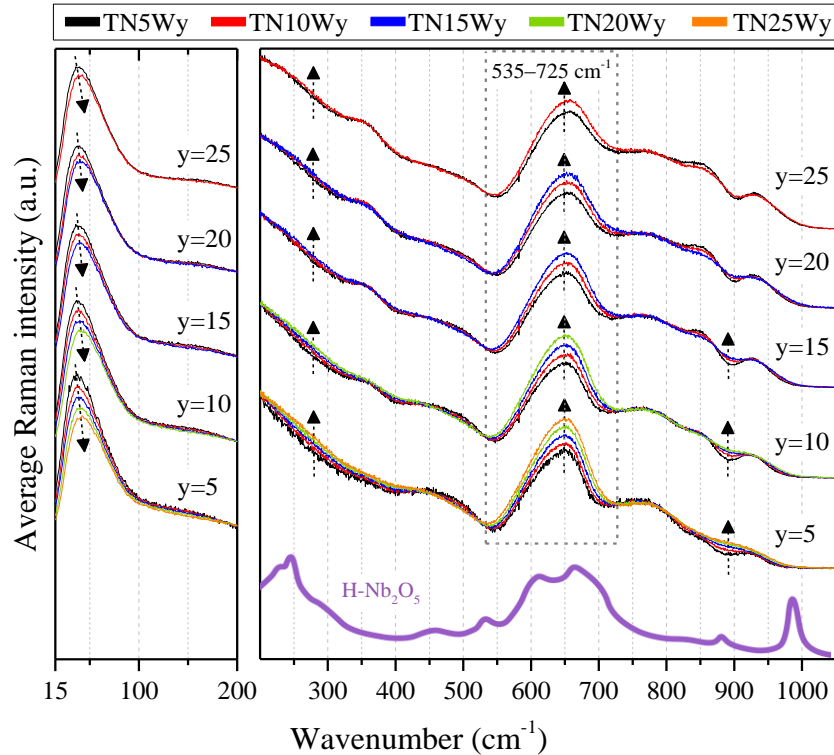


Fig. 3. Evolution of total-area averaged Raman spectra of TN_xW_y glasses as a function of NbO_{2.5} content. The low-wavenumber (boson peak) and mid- to high-wavenumber regions are supplied apart for more clarity. The Raman spectrum of H-Nb₂O₅ is reproduced from Fig. 34 in [34].

For a more accurate structural analysis, we used the conventional spectral decomposition technique based on the addition of bands of which the position (wavenumber), width (more precisely the full-width at half maximum, FWHM) and intensity can be either assigned fixed values or left free (unconstrained). In wavenumber regions where band shift and/or broadening are observed with increasing NbO_{2.5} (or WO₃) content, we kept the introduced function's wavenumber and/or FWHM respectively parameter-free. Thus, the bands A, H and M were fully unconstrained, while bands F and L were introduced with fixed FWHM values

and bands D and J with fixed wavenumbers values. The remaining bands B, C, E, G, I and K were introduced with fixed wavenumber and FWHM values.

The origins of bands associated with vibrations of Te–O bonds (bands E–J) are supported by pioneer works on the vibrational and structural properties of the three TeO₂ polymorphs (α [58], β [58] and γ [59]). The origins of the bands involving vibrations of Nb–O bonds (bands E, G, H and M) are based on the structural studies of Nb₂O₅ and binary TeO₂-Nb₂O₅ crystals (*cf.* Table 2 for a detailed band assignment). The basis of the vibrational mode assignment of distorted WO₆ octahedra is a bilateral analysis of the vibrational (Raman spectra) *vs.* structural features that we conducted on a large number of tungsten-containing oxides (metal tungstates for the most part). A similar approach has been previously undertaken on few tungstates by Sekiya *et al.* [25]. The obtained decomposition results (calculated parameters for the inserted bands) were used to evaluate the areas of each band in all of the decomposed spectra. Then, the normalized intensity of each band was calculated by dividing the band area by the molar content(s) of the oxide(s) of which the constituent ionic species are responsible for that vibration.

3.3.1. Structural effect of adding NbO_{2.5}

The recorded Raman spectra from TN_xW₅ glasses are provided in Fig. 4. At first glance, one can notice the important change in the $\sim 535\text{-}725\text{ cm}^{-1}$ range with a noticeable intensity increase of the bands G and H from TN₅W₅ to TN₂₅W₅. Slight increasing of Raman intensity is observed within $\sim 200\text{-}400\text{ cm}^{-1}$ and $\sim 850\text{-}950\text{ cm}^{-1}$ regions. On the other hand, in the low-wavenumber region ($< 100\text{ cm}^{-1}$), an intensity decrease of the boson peak is recorded along with an insignificant red-shift of $\sim 6\text{ cm}^{-1}$ from TN₅W₅ to TN₂₅W₅.

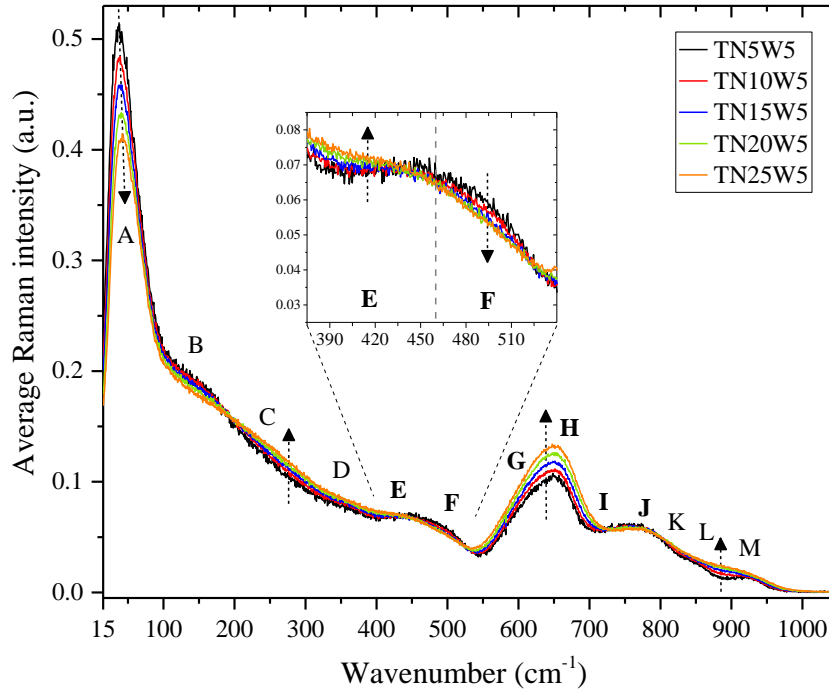


Fig. 4. Total-area averaged Raman spectra of TN_xW₅ glasses. The labels A–M correspond to the inserted bands for the spectral decomposition. Inset: zoom of the region 375-540 cm⁻¹.

As explained in the introduction of section 3.3, we have calculated, for each TN_xW_y composition, the normalized intensities of bands E, G and H by dividing their areas by the sum of TeO₂ and NbO_{2.5} molar contents; those of bands F, I and J by dividing their areas by TeO₂ content. The compositional dependence of the normalized intensities in TN_xW₅ glasses is plotted in Fig. 5. Similar band evolutions are observed in other sets of TN_xW_y samples at constant WO₃ content and increasing NbO_{2.5} content.

Let us now focus on the decomposition results as a function of NbO_{2.5} content from the mid- to high-wavenumber range 400-1000 cm⁻¹.

- ***In the 400-550 cm⁻¹ region:***

As can be seen in the inset of Fig. 4, the intensities of the two bands E and F seem to evolve in opposite directions. It can be seen from Fig. 5 that while the normalized intensity of band E slightly increases by ~10%, the band F remains practically constant. Taking into account the

compositional evolutions of the two bands E and F, we argue that continuous adding of NbO_{2.5} results in an increase of the number of Te–O–Nb and/or nearly symmetric Te–O–Te bridges (as in γ -TeO₂).

Inserted band	Wavenumber (cm ⁻¹)	Raman band assignments
A	36.0 – 39.8	• The boson peak, ascribed to an excess density of vibrational states [60].
B	146.9 (<i>fixed</i>)	• Intra-chain vibrations of Te–Te bonds (as in amorphous t-Te) [61].
C	243.6 (<i>fixed</i>)	• Bending vibrations of WO ₆ octahedra (as in γ -WO ₃) [62].
D	351 (<i>fixed</i>)	• Bending vibrations of distorted WO ₆ octahedra [62].
E	425 (<i>fixed</i>)	<ul style="list-style-type: none"> • Symmetric stretching vibrations in nearly symmetric Te–O–Te bridges (as in γ-TeO₂) [58,59]. • Symmetric stretching vibrations of Te–O–Nb bridges (as in Nb₂Te₄O₁₃ and Nb₂Te₃O₁₁ [34]).
F	497.3 – 522	• Symmetric stretching vibrations in Te–O–Te bridges [58,59].
G	607 (<i>fixed</i>)	<ul style="list-style-type: none"> • Asymmetric stretching vibrations in nearly symmetric Te–O–Te bridges (as in γ-TeO₂) [58,59]. • Stretching vibrations of highly asymmetric and almost terminal Te–O– – –Nb linkages [34]. • Stretching vibrations of Nb–O in Nb–O–Nb bridges (as in H-Nb₂O₅ [34]).
H	658.8 – 661.1	<ul style="list-style-type: none"> • Asymmetric stretching vibrations in asymmetric Te–O–Te bridges [58,59]. • Stretching vibrations of highly asymmetric and almost terminal Te–O– – –Nb linkages [34]. • Stretching vibrations of Nb–O in Nb–O–Nb bridges (as in H-Nb₂O₅ [34]).
I	715 (<i>fixed</i>)	<ul style="list-style-type: none"> • Asymmetric stretching vibrations in asymmetric Te–O–Te bridges [58,59]. • Symmetric stretching vibrations in W–O–W bridges (as in γ-WO₃) [62].
J	772 (<i>fixed</i>)	• Asymmetric stretching of essentially covalent Te–_{eq}O bonds [58,59].
K	820 (<i>fixed</i>)	• Asymmetric stretching vibrations in W–O–W bridges (as in γ -WO ₃) [62].
L	852.3 – 845.9	• Stretching vibrations of W–O bonds in W–O–W bridges.
M	920.4 – 898.5	<ul style="list-style-type: none"> • Asymmetric stretching vibrations of W–O bonds [62]. • Stretching vibrations of the shortest Nb–O bonds [34].

Table 2. Wavenumbers and vibrational assignments of the inserted bands. Raman bands arising from TeO₂ network and their assignments are highlighted in bold typeface. In the spectral decomposition process, the wavenumbers of A, F, H, L and M bands were unconstrained and are given herein as wavenumber ranges from the set of TNxW5 glasses with increasing x.

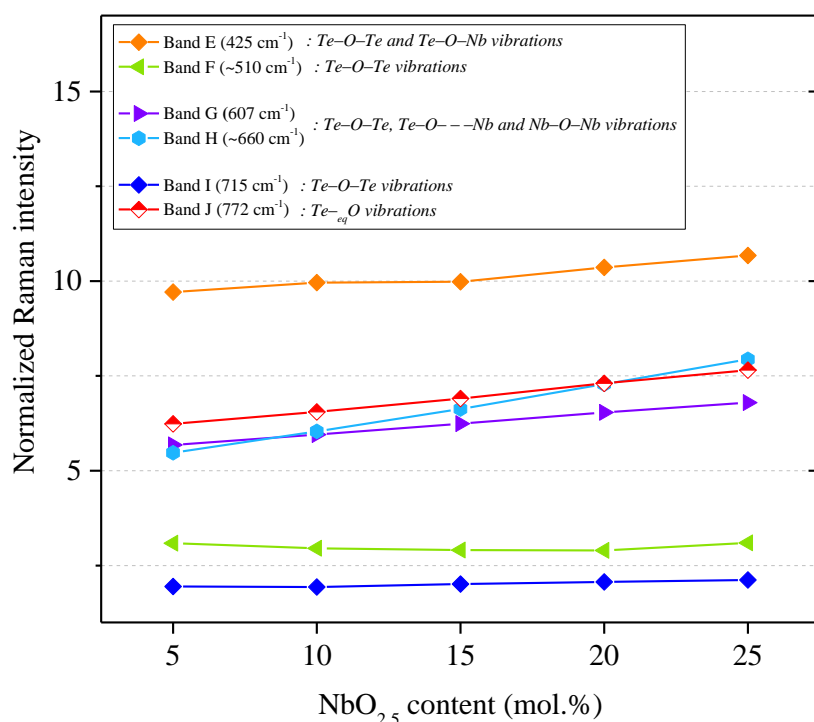


Fig. 5. Compositional dependence of the normalized intensities of inserted bands for spectral decomposition of TNxW5 glasses. The areas of bands E, G and H were divided by the sum of TeO₂ and NbO_{2.5} contents; those of bands F, I and J by the TeO₂ content.

- ***In the 550-800 cm⁻¹ region:***

The normalized intensities of bands G and H increase by ~20% and ~45% respectively upon adding NbO_{2.5} (Fig. 5). To appropriately interpret the structural trend based on the evolution of these two bands, it is important to consider the shape of the corresponding Raman band (within the range of 535-725 cm⁻¹, cf. Fig. 3). A simple visual analysis indicates that its intensity increases upon adding NbO_{2.5} with no apparent band shift. From the viewpoint of the TeO₂-rich network in TNxW5 glasses, the fact that this large band does not red-shift might renounce any significant structural depolymerization. In the opposite case, *i.e.*, when a modifier oxide such as Tl₂O with a weak modifier cation Tl⁺ is added to the TeO₂-rich network, a significant red-shift of this band is observed due to the simultaneous intensity decrease of the Raman band assigned to Te–O bond vibrations in TeO₄ units (in the ~607-772 cm⁻¹ range) and increase of the one assigned to Te–O bond vibrations in TeO₃ units (in the

~660-715 cm⁻¹ range) [63]. It is important to note that the stretching vibrations of Nb–O–Nb bridges are also observed in the 535-725 cm⁻¹ range (*cf.* Raman spectrum of H-Nb₂O₅ in Fig. 3). Regarding the evolutions of bands I and J, their normalized intensities show marginal and stronger upward (increase by ~23%) trends respectively (Fig. 5). Therefore, we argue that the evolution of bands G–J probably suggests both a slight structural depolymerization of the Te–O–Te bond network and/or increasing number of Nb–O–Nb and/or Te–O–Nb bridges.

It is relevant to assess the evolution of Raman band ratios corresponding to the two ultimate TeO₄ and TeO₃ structural units. In this spirit, Ghribi *et al.* [64] suggested to gauge the depolymerization extent (ratio of TeO₃/TeO₄) as a function of ZnO content in TeO₂-TiO₂-ZnO glasses by calculating the following ratio of normalized intensities: $(I_H + I_I)/(I_G + I_H + I_J)$ where the numerator holds the sum of intensity relative to bands due to stretching vibrations of Te–O in TeO₃ units, and denominator to those in TeO₄ units. We have calculated this ratio in TNxW5 glasses and the obtained results are illustrated in Fig. 6. It is important to stress that the ratio values do not quantitatively reflect the ratio of TeO₃/TeO₄ but rather a qualitative evolution. This can be explained by the following reasons: (i) the Raman intensity is proportional to both the number of vibrating entities and the extent of the polarizability change; and (ii) it is complicated to sharply distinguish TeO₃ from TeO₃₊₁ and TeO₄ units as there are no clear-cut boundaries due to a large panel of slightly distinct intermediate units demonstrating broad distributions of Te–O bond lengths.

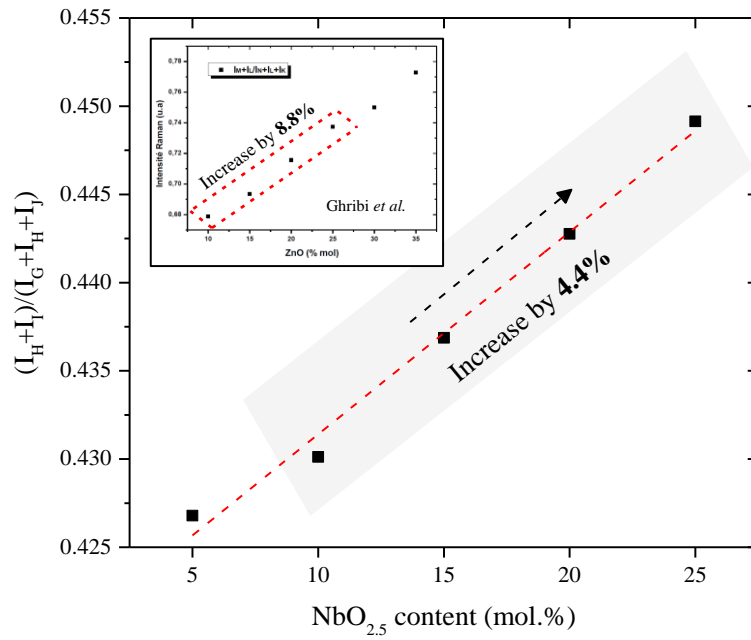


Fig. 6. Evolution of the ratio of normalized intensities $(I_H + I_I)/(I_G + I_H + I_I)$ in TNxW5 glasses. Inset: evolution of the same ratio in $(95-y)\text{TeO}_2-5\text{TiO}_2-y\text{ZnO}$ glasses as a function of ZnO content as reported by Ghribi *et al.* [64].

The observed increase of the ratio $(I_H + I_I)/(I_G + I_H + I_I)$ in TNxW5 glasses might indicate a slight transformation of TeO_4 into TeO_3 structural units. It is important to emphasize that this ratio increase in our TNxW5 glasses (by 4.4% from 10 to 25 mol.% $\text{NbO}_{2.5}$) is twice weaker than in $(95-y)\text{TeO}_2-5\text{TiO}_2-y\text{ZnO}$ glasses upon adding ZnO from 10 to 25 mol.% (*cf.* inset in Fig. 6). This suggests that the structural effect of $\text{NbO}_{2.5}$ in depolymerizing the Te–O–Te bond network of TNxW5 glasses is weaker than that of ZnO; and very likely much weaker than the influence of alkali or alkaline-earth oxides which strongly induce the structural depolymerization of TeO_4 units into TeO_3 ones. Therefore, it can be argued that $\text{NbO}_{2.5}$ has only a weak depolymerizing effect on the TeO_2 -rich network by transforming TeO_4 into TeO_{3+1} and TeO_3 units.

From the evolution of the Nb–O–Nb bond network, increasing the $\text{NbO}_{2.5}$ content from 5 to 25 mol.% results in an increase of the number of $\text{NbO}_{2.5}$ -rich regions until the crystallization of $\text{Nb}_6\text{TeO}_{17}$ [56] at 30 mol.% of $\text{NbO}_{2.5}$. The structure of this compound has not been

determined yet; however, given the high NbO_{2.5}:TeO₂ ratio (6:1), one can predict the predominant contribution of Nb–O–Nb bridges in its crystal lattice. This shifting behavior of NbO_{2.5} from a network modifier towards a network former as manifested by the presence of NbO_{2.5}-rich regions is in agreement with the obtained results from TeO₂-NbO_{2.5} glasses by Hoppe *et al.* [40].

- ***In the 800-1000 cm⁻¹ region:***

It should be noted that the intensity of the “shoulder” centered at ~880 cm⁻¹ (*cf.* Fig. 3) which is due to stretching vibrations of the shortest (terminal) Nb–O bonds increases but very moderately with NbO_{2.5}. This means that its expected normalized intensity must rather decrease since adding twice more NbO_{2.5} (*e.g.*, from 5 to 10 mol.%) does not yield twice more intense response in this region. This suggests that less and less terminal Nb–O bonds exist at the expense of Nb–O–Nb (bands G and H) and Te–O–Nb (band E) bridges. This is in total agreement with the previously discussed evolution of these two varieties of bridges, *i.e.*, their number increase upon adding NbO_{2.5}. We omitted in Fig. 5 the evolution of the normalized intensity of this shoulder centered at ~880 cm⁻¹ for the two following reasons: (*i*) the shoulder is strongly overlapping with the surrounding bands L and M, and (*ii*) due to the influence of the band M (also due to the asymmetric stretching vibrations of W–O bonds) of which the normalized intensity changes as a function of the molar ratio of TeO₂ to WO₃ [43].

To sum up, we argue that the structural effect of NbO_{2.5} is simultaneously manifested by (*i*) the weak structural depolymerization of Te–O–Te bond network and (*ii*) the existence of NbO_{2.5}-rich regions upon adding NbO_{2.5} through increasing Te–O–Nb and Nb–O–Nb bridges.

3.3.2. Structural effect of adding WO₃

The recorded Raman spectra of TN_xW_y glasses with increasing WO₃ content are presented in Fig. 7. The evolving band features are in agreement with the reported studies on TeO₂-based glasses containing WO₃ by Raman spectroscopy [25,30,65], *i.e.*, three additional bands at ~360, ~860 and ~925 cm⁻¹ appear at the Raman spectra and increase in intensity upon adding WO₃. Since close tendencies are observed in TN_xW_y sets of glasses at different NbO_{2.5} contents, we suggest to examine the structural evolution in TN5W_y glass series. The obtained decomposition results for TN5W_y glasses are given below in Fig. 8. Very close trends have been previously observed from glasses within the TeO₂-TiO₂-WO₃ system and more details on this structural analysis can be found in [43].

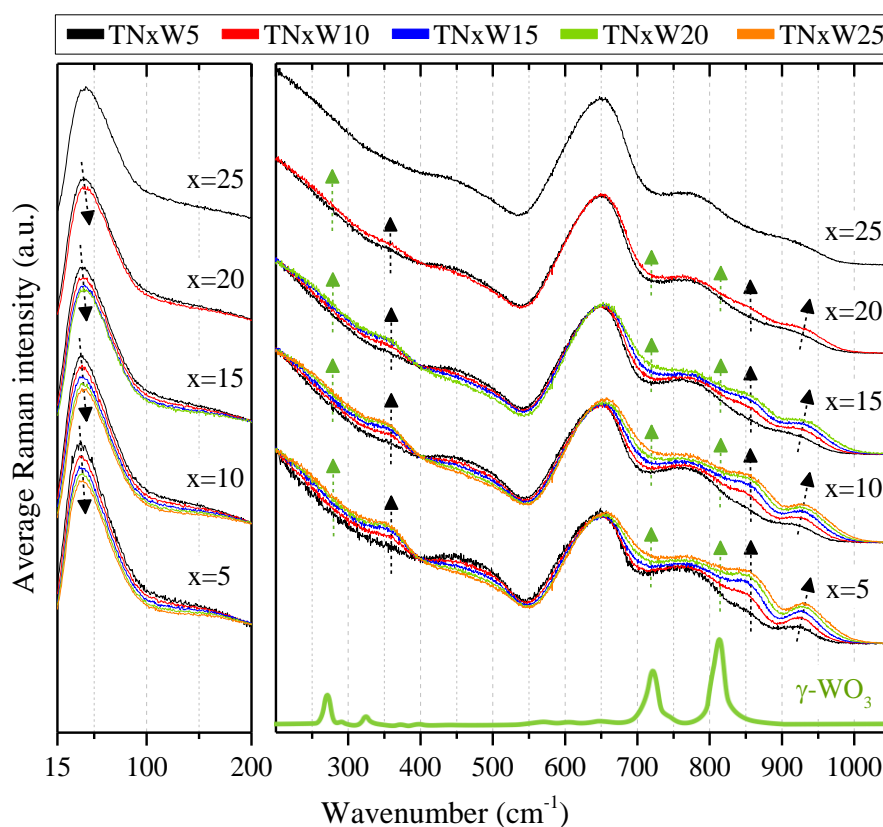


Fig. 7. Evolution of total-area averaged Raman spectra of TN_xW_y glasses as a function of WO₃ content. The Raman spectrum of γ -WO₃ is reproduced from Figure 2 in [62].

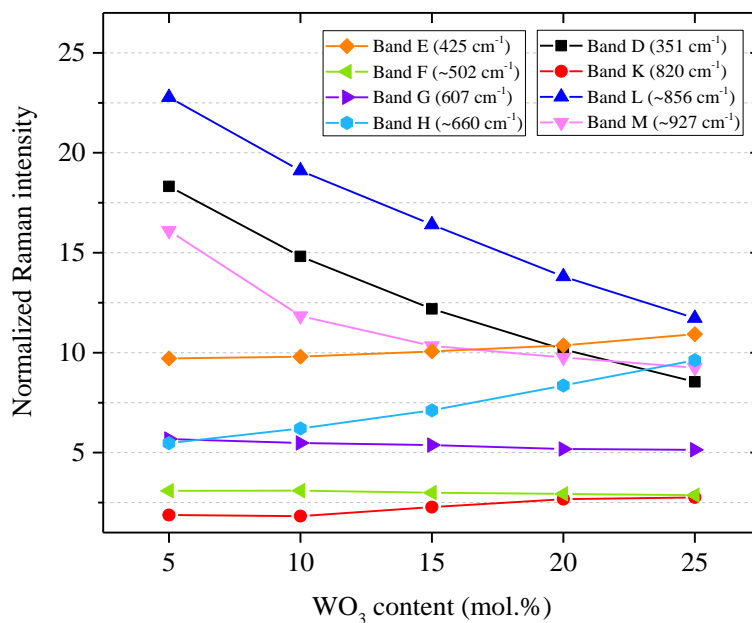


Fig. 8. Compositional dependence of the normalized intensities of inserted bands for spectral decomposition of TN₅W_y glasses. The areas of bands E–H were divided by the TeO₂ content; those of bands D and K–M by the WO₃ content.

The evolutions of the normalized intensities of bands E–G suggest a minor structural modification of the bond network of TN_xW_y glasses. While the bands F and G remain practically constant upon adding WO₃, the band E shows a slight increase of its normalized intensity that might be associated with a slightly increasing number of nearly symmetric Te–O–Te bridges. The increasing normalized intensity of the band H (assigned to asymmetric stretching vibrations in asymmetric Te–O–Te bridges) is the result of its broadening due to a number increase of W–O–W bridges in the glass network upon adding WO₃, which complicates the interpretation of this band. The evolutions of the normalized intensities of bands D and K–M suggest a progressively reducing number of uniformly dispersed WO₆ octahedra at the expense of WO₃-rich regions with increasing WO₃ content as previously suggested in binary TeO₂–WO₃ by Sekiya *et al.* [25]. Moreover, it is important to note the slight red-shift, upon adding WO₃, of the band M assigned to the stretching vibrations of terminal W–O bonds in WO₆ octahedra.

Lastly, regarding the evolution of the band A (boson peak), the position of its maximum intensity insignificantly red-shifts accompanied with an intensity decrease with addition of NbO_{2.5} or WO₃ contents (Fig. 3 and Fig. 7). According to literature [60,66], the evolution of boson peak's position and intensity in TN_xW_y glasses could suggest a slight crosslinking density increase in the glass network at the medium-range scale. This behavior is in agreement with the continuous increase of the glass transition temperature upon adding NbO_{2.5} or WO₃.

3.4. Optical properties

3.4.1. Linear optical properties

3.4.1.1. Refractive index, optical band gap and Urbach energies by UV-Vis-NIR spectroscopy

We recorded the optical transmission spectra from TN_xW_y glass pellets over a wide wavelength range extending from 300 to 3300 nm (Fig. 9). The optical transmission spectra of 16 out of 17 glass samples show a transparency over 75% in the 800-2600 nm range. The exception is the sample TN5W5 showing a slightly lower transparency of ~73%, which might be due to its peculiar composition (richest in TeO₂) at the boundary of the glass-forming domain. The absorption band onsetting at 2800 nm corresponds to the stretching mode of bound hydroxyl groups (R-OH), and symmetric and asymmetric stretching modes of water molecules [67]. The transmission percentage is neither enhanced nor reduced upon adding NbO_{2.5} but rather fluctuates within a relatively narrow range of less than 2% (Fig. 9). This is also the case with increasing WO₃ content (*cf.* Fig. 10 for TN5W_y glasses).

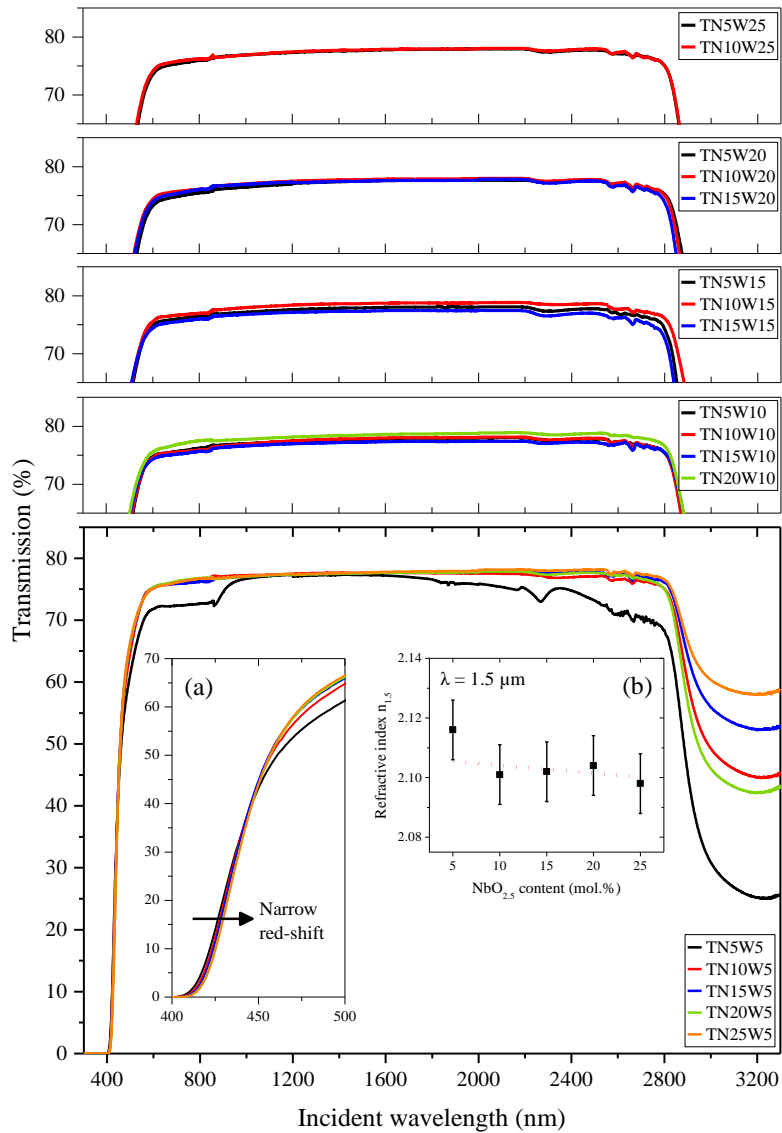


Fig. 9. UV-Vis-NIR spectra of TN_xW_y glasses. Insets for TN_xW₅: (a) Zoom-in plot of the UV absorption edge. (b) Compositional dependence of the refractive index $n_{1.5}$ calculated at $1.5 \mu\text{m}$.

The linear refractive indices were extracted from the optical transmission data at $\lambda = 1.5 \mu\text{m}$ using the following equation: $T = 2n/(n^2+1)$. The refractive indices $n_{1.5}$ are listed in Table 1. Generally, the obtained results suggest a practically constant behavior of the refractive index upon adding either NbO_{2.5} or WO₃ with high values ranging approximately from 2.06 to 2.12. It should be stressed that because of the Fresnel reflection at the air-glass interface, the above equation slightly underestimates the actual refractive index value, which will then be provided from ellipsometric measurements.

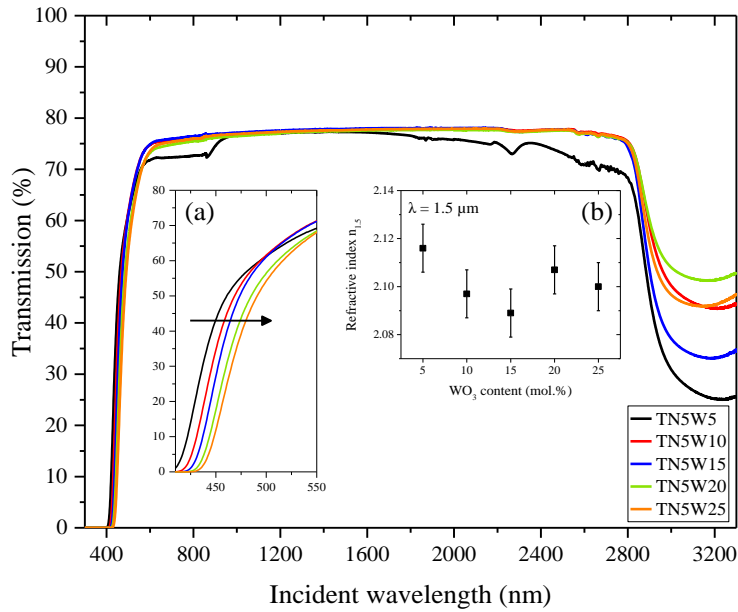


Fig. 10. UV-Vis-NIR optical transmission spectra of TN5Wy glasses. Insets: (a) Zoom-in plot of the UV absorption edge. (b) Compositional dependence of the refractive index $n_{1.5}$ calculated at 1.5 μm .

The UV absorption edge slightly shifts towards longer wavelengths within the range of 410-415 nm upon adding $NbO_{2.5}$ in $TNxW5$ glasses (Fig. 9), implying a gradual slight decrease of the optical band gap energy E_g . Upon adding WO_3 (Fig. 10), a stronger red-shift is observed within a larger wavelength range (400-437 nm). The color evolution of glasses (*cf.* section 3.1) is in agreement with the noticed shift of the absorption edge.

Both the optical band gap E_g and Urbach E_U energies were extracted from the UV absorption edges of $TNxWy$ glasses. Based on the wavelength-dependence of the approximate absorption coefficient α (estimated using the expression $\alpha(\lambda) = (1/d) \ln(T_{\text{max}}/T(\lambda))$, where T is the transmission percentage and d is the sample thickness), we plotted $(\alpha h\nu)^{1/2}$ versus the incident photon energy $h\nu$ (commonly known as Tauc plot) to estimate E_g (Fig. 11). The E_g values lie in the range of 2.77–2.92 eV (Table 1). Adding $NbO_{2.5}$ from 5 to 25 mol.% in $TNxW5$ glasses results in a steady evolution of E_g from 2.92 eV to 2.89 eV. On the other hand, adding WO_3 induces a slight decrease of 5% from TN5W5 (2.92 eV) to TN5W25 (2.78

eV). These evolutions of E_g upon adding $\text{NbO}_{2.5}$ and WO_3 are in agreement with the literature on the $\text{TeO}_2\text{-Nb}_2\text{O}_5$, $\text{TeO}_2\text{-ZrO}_2\text{-WO}_3$ and $\text{TeO}_2\text{-BaO-Nb}_2\text{O}_5$ systems [32,68,69].

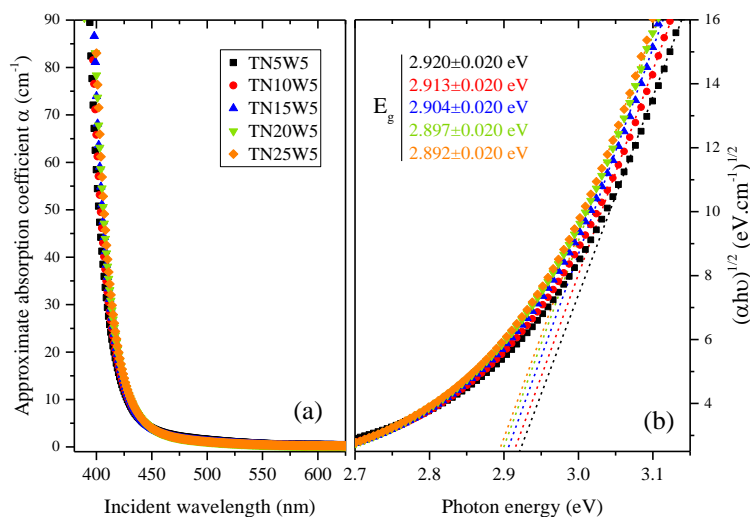


Fig. 11. (a) Evolution of the approximate absorption coefficient α as a function of the incident wavelength in TN_xW_5 glasses. (b) Tauc plot for the optical band gap energy E_g derived from the absorption coefficient in TN_xW_5 glasses.

The extracted values of Urbach energy E_U lie in the range 0.104-0.114 eV for all the compositions. E_U remains fairly stable with increasing WO_3 content (*e.g.*, 0.109 eV in TN5W_y glasses). However, a slight decrease from 0.114 to 0.105 eV is observed upon adding $\text{NbO}_{2.5}$ from TN5W_5 to TN25W_5 . E_U is characteristic of the width of the band-tails thus estimating the density of localized states [70]. A highly disordered glass network is characterized by a higher density of localized states and thus having a high E_U value. These values are very close to those reported in literature for $\text{NbO}_{2.5}$ - and WO_3 -containing TeO_2 -based glasses (ranging between 0.096 and 0.114 eV, see *e.g.*, [46]). Therefore, it can be argued that adding $\text{NbO}_{2.5}$ might slightly lessen the overall structural disorder of the glass network.

3.4.1.2. Refractive index dispersion by spectroscopic ellipsometry

We measured the wavelength-dispersion of the refractive index from TNxWy glass pellets in the range of 350-830 nm (*cf.* Fig. 12 for TNxW5 glasses), and derived the refractive indices n_∞ (Table 1) extrapolated to infinite wavelength using Sellmeier's dispersion formula [71,72]: $n = (A + B/(1-C/\lambda^2) + D/(1-E/\lambda^2))^{1/2}$ where A–E are fitting constants specific to each sample. An excellent fitting quality was achieved as demonstrated by the R^2 coefficients ranging between 0.9970 and 0.9999. The studied glasses collectively exhibit high n_∞ indices with an average of ~ 2.13 ($n_{\infty(\min)} = 2.12$ and $n_{\infty(\max)} = 2.15$) which is ~ 1.5 times higher than the refractive index of SiO₂ glass (1.439 at 1.9 μm [53]) and practically equal to that of TeO₂ glass (2.121 at 1.9 μm [53]).

The dependence of n_∞ on the WO₃ content suggests a constant behavior with an average value of ~ 2.14 in TNxW5 and TNxW25 glass series. Likewise, it seems that n_∞ remains practically constant upon adding NbO_{2.5} with average values of ~ 2.13 in TN5Wy glasses and ~ 2.15 in TN25Wy (corresponding to the unique TN25W5 sample). A similar steady evolution of the refractive index in binary (100-x)TeO₂-xWO₃ and (100-x)TeO₂-xNbO_{2.5} glasses was reported [45] with values in the ranges of 2.21-2.19 and 2.21-2.22 with increasing WO₃ and NbO_{2.5} contents from 10 to 30 mol.%, respectively. With an average of 2.13 for TNxWy glasses, the n_∞ value is $\sim 3\%$ lower than those reported for the above binary glasses and that extracted from TeO₂-TiO₂-WO₃ glasses ($n_{\infty(\text{average})}$ of 2.192) [43]. It is important to stress that the n_∞ values reported here are higher in comparison to other binary or ternary systems where a more consequential structural depolymerization occurs upon modifying the glass network (*e.g.*, less than 2.100 in TeO₂-TiO₂-ZnO glasses [64]).

Finally, the steady evolutions of the extracted refractive indices for TNxWy glasses from both optical transmission ($n_{1.5}$) and ellipsometry (n_∞) measurements are in good agreement.

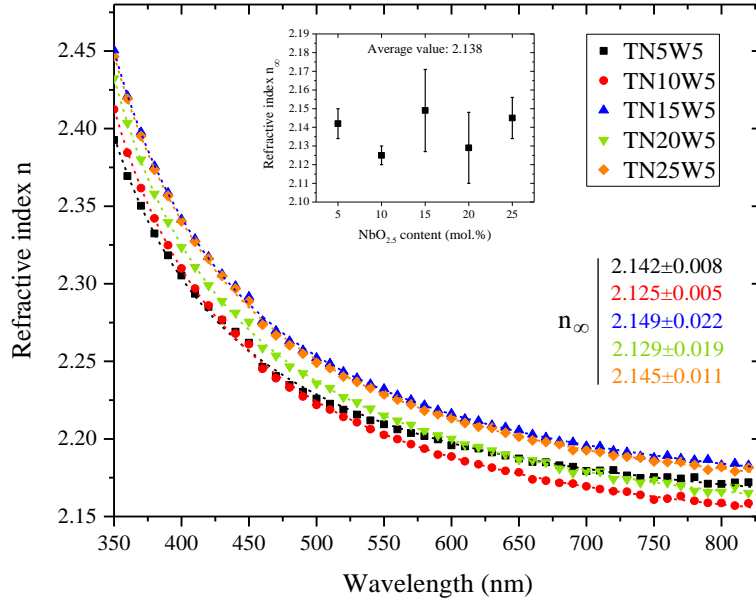


Fig. 12. Wavelength dispersion of the refractive index dispersion for TNxW5 glasses. Each dispersion curve corresponds to the average of three measured curves from different spots on the same glass pellet. Inset: Compositional dependence of the refractive index.

3.4.2. Nonlinear optical properties

As described in the experimental section, the third-order nonlinear susceptibilities $\chi^{(3)}$ have been measured using the Z-scan technique at $\lambda = 800$ nm. From the measured Z-scan transmittance curves, the extracted peak-valley transmittance change ΔT_{p-v} (example of TN15W20 in Fig. 13) is used to derive the $\chi^{(3)}$ values from the TNxWy glass pellets (*cf.* Table 1, with $\chi^{(3)}_{\min} = 4.75 \cdot 10^{-13}$ esu and $\chi^{(3)}_{\max} = 6.38 \cdot 10^{-13}$ esu). Interestingly, the average $\chi^{(3)}$ value of $5.48 \cdot 10^{-13}$ esu among TNxWy glasses is ~ 37 times higher than the $\chi^{(3)}$ value of SiO₂ glass ($0.15 \cdot 10^{-13}$ esu [52]) and slightly lower than that of pure TeO₂ glass ($7.54 \cdot 10^{-13}$ esu).

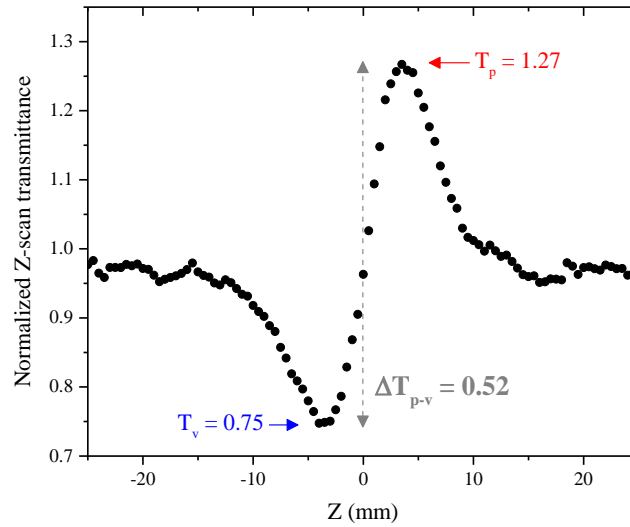


Fig. 13. Example of a measured Z-scan curve from the TN15W20 glass sample.

The compositional dependence of $\chi^{(3)}$ values in TN x W y glasses upon adding NbO $_{2.5}$ or WO $_3$ can be found in Fig. 14. Their evolution upon adding NbO $_{2.5}$ suggests a fairly constant behavior from $\sim 5.2 \cdot 10^{-13}$ esu in TN5W y to $\sim 5.1 \cdot 10^{-13}$ esu in TN25W y . Likewise, adding WO $_3$ seems to maintain the $\chi^{(3)}$ values practically stable. It is worthwhile to mention that the binary (100- x)TeO $_2$ - x NbO $_{2.5}$ glasses exhibit higher $\chi^{(3)}$ values ranging from $7.540 \cdot 10^{-13}$ esu ($x = 10$ mol.%) to $9.037 \cdot 10^{-13}$ esu ($x = 30$ mol.%) [1].

The overall evolution of the nonlinear response of TN x W y glasses upon substituting TeO $_2$ with either NbO $_{2.5}$ or WO $_3$ is shown in Fig. 15. This positive contribution could be explained by the possible influence of empty d -orbitals of each of Nb $^{5+}$ and W $^{6+}$ cations via virtual electronic transitions to d -orbitals and to the conduction band sp -orbitals as reported by Lines [73]. Nevertheless, it is very important to keep in mind that these derived values and discussed evolutions could be tempered considering the significant error bars of $\sim 20\%$ in average for the $\chi^{(3)}$ responses: in concrete terms, the $\chi^{(3)}$ evolutions could be regarded as practically steady as well.

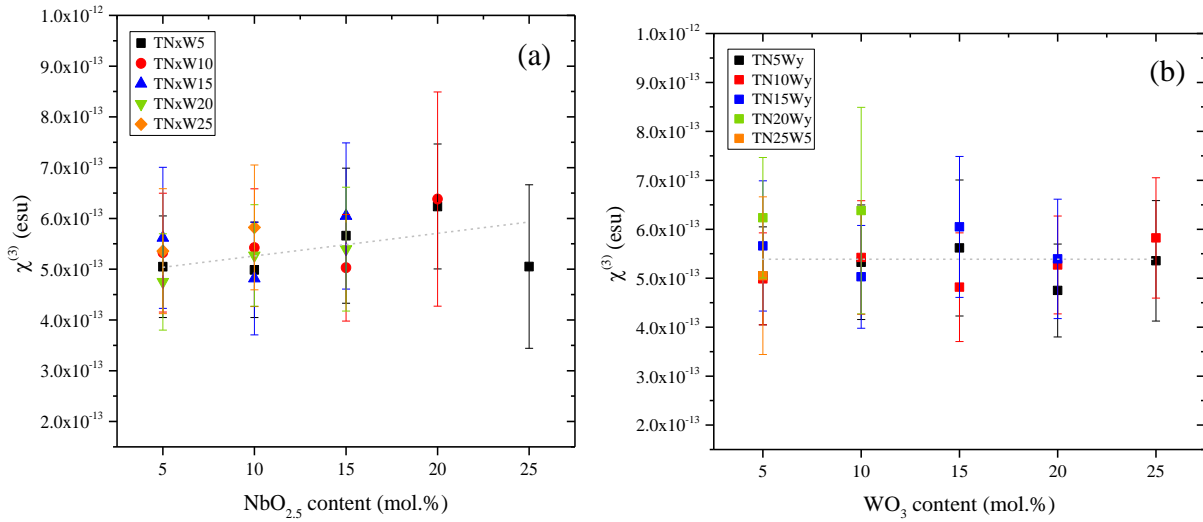


Fig. 14. Evolution of normalized $\chi^{(3)}$ values as a function of (a) $\text{NbO}_{2.5}$ and (b) WO_3 contents.

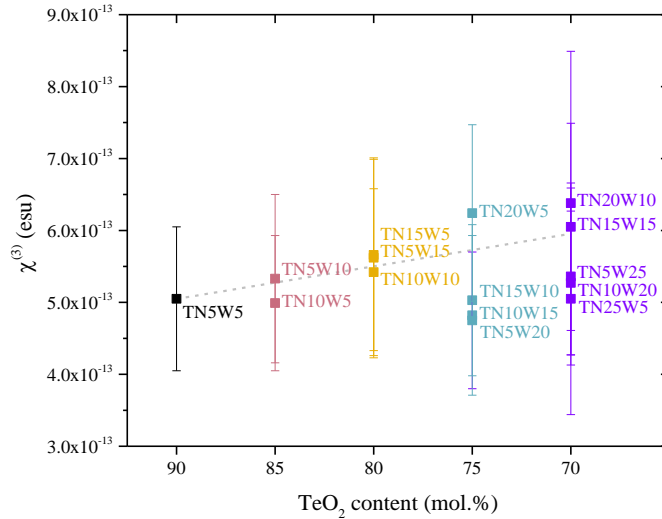


Fig. 15. Evolution of normalized $\chi^{(3)}$ values as a function of TeO_2 content.

Generally, the evolution of the nonlinear optical performance of TN_xW_y glasses is consistent with the structural interpretations established in section 3.3.1 suggesting that only relatively slight modifications occur throughout the glass network with addition of either $\text{NbO}_{2.5}$ or WO_3 . The steady evolution of $\chi^{(3)}$ values upon adding $\text{NbO}_{2.5}$ or WO_3 highly suggests the absence of any striking structural depolymerization of the Te-O-Te bond network.

4. Conclusions.

A systematic study within the $(100-x-y)\text{TeO}_2-x\text{NbO}_{2.5}-y\text{WO}_3$ glassy system has been established for the first time. The glass-forming domain, density, thermal, structural and optical (linear and nonlinear) properties of these glasses have been investigated and analyzed as a function of $\text{NbO}_{2.5}$ and WO_3 contents. The explored glass-forming domain holds seventeen compositions and extends from $x = 5$ to 25 mol.% in $\text{NbO}_{2.5}$ and $y = 5$ to 25 mol.% in WO_3 . The studied TN_xW_y glasses exhibit moderate thermal stabilities ($\Delta T_{(\text{min})} = 45$ °C and $\Delta T_{(\text{max})} = 70$ °C) and glass transition temperatures that increase with addition of $\text{NbO}_{2.5}$ and WO_3 ($T_{g(\text{min})} = 333$ °C and $T_{g(\text{max})} = 403$ °C).

Based on the undertaken structural analysis established from full-scale Raman spectral decomposition, we report the following trends:

- The structural effect of incorporating $\text{NbO}_{2.5}$ is manifested in both (i) a weak structural depolymerization of the Te–O–Te bond network accompanied by an increasing number of Te–O–Nb and/or Nb–O–Nb bridges and (ii) existence of $\text{NbO}_{2.5}$ -rich regions upon continuous addition of $\text{NbO}_{2.5}$ until the crystallization of $\text{Nb}_6\text{TeO}_{17}$ compound which corresponds to a high $\text{NbO}_{2.5}:\text{TeO}_2$ ratio of 6:1.
- Adding WO_3 results, at low WO_3 contents, in uniformly dispersed WO_6 octahedra throughout the glass network, and at higher WO_3 contents, in amorphous “ WO_3 -rich” regions that continuously grow prior to the crystallization of $\text{WO}_{2.83}$ in TN_xW_30 samples. This idea is in agreement with the one proposed by Sekiya *et al.* [25] and recently highlighted in the $\text{TeO}_2\text{-TiO}_2\text{-WO}_3$ glassy system [43].

The revealed structural properties are consistently correlated to the measured optical (linear and nonlinear) properties. The studied TN_xW_y glasses exhibit high linear refractive indices ($n_{\infty(\text{min})} = 2.12$ and $n_{\infty(\text{max})} = 2.15$) with an average n_{∞} of 2.13 which is ~ 1.5 times higher than

the refractive index of SiO₂ glass. It is found that the measured n_{∞} values remain practically constant upon adding either NbO_{2.5} or WO₃.

The extracted third-order nonlinear susceptibilities $\chi^{(3)}$ values are very high ($\chi^{(3)}_{\min} = 4.75 * 10^{-13}$ esu and $\chi^{(3)}_{\max} = 6.38 * 10^{-13}$ esu) with an average of $5.48 * 10^{-13}$ esu that is ~37 times stronger than the reported $\chi^{(3)}$ value for SiO₂ glass. Moreover, they are found to remain practically steady with addition of NbO_{2.5} and WO₃: from TN5Wy ($5.22 * 10^{-13}$ esu) to TN25Wy ($5.05 * 10^{-13}$ esu), and from TNxW5 ($5.40 * 10^{-13}$ esu) to TNxW25 ($5.59 * 10^{-13}$ esu) respectively. Generally, the extracted $\chi^{(3)}$ values from TNxWy glasses are higher than those reported from other TeO₂-based systems and particularly those where a significant structural depolymerization takes place (*e.g.*, ZnO- or alkali-containing glasses).

Acknowledgements.

M.R. Zaki gratefully acknowledges the financial support from Conseil Régional du Limousin. The authors acknowledge the financial support from the CNRS via the "Projet International de Coopération Scientifique (PICS)" No. 7257 and would also like to thank Dr. J. Cornette and Dr. R. Mayet for their valued technical assistance in data acquisition of Raman spectra and XRD patterns respectively.

References.

- [1] S.-H. Kim, T. Yoko, Nonlinear optical properties of TeO₂-based glasses: MO_x-TeO₂ (M= Sc, Ti, V, Nb, Mo, Ta, and W) binary glasses, *J. Am. Ceram. Soc.* 78 (1995) 1061–1065. doi:10.1111/j.1151-2916.1995.tb08437.x.
- [2] V. Dimitrov, S. Sakka, Linear and nonlinear optical properties of simple oxides. II, *J. Appl. Phys.* 79 (1996) 1741–1745. doi:10.1063/1.360963.
- [3] R.A.H. El-Mallawany, *Tellurite glasses handbook: physical properties and data*, 2nd ed, Taylor & Francis, Boca Raton, FL, 2011.
- [4] A. Jha, B.D.O. Richards, G. Jose, T. Toney Fernandez, C.J. Hill, J. Lousteau, P. Joshi, Review on structural, thermal, optical and spectroscopic properties of tellurium oxide based glasses for fibre optic and waveguide applications, *Int. Mater. Rev.* 57 (2012) 357–382. doi:10.1179/1743280412Y.0000000005.
- [5] J. Massera, A. Haldeman, D. Milanese, H. Gebavi, M. Ferraris, P. Foy, W. Hawkins, J. Ballato, R. Stolen, L. Petit, K. Richardson, Processing and characterization of core–clad tellurite glass preforms and fibers fabricated by rotational casting, *Opt. Mater.* 32 (2010) 582–588. doi:10.1016/j.optmat.2009.12.003.
- [6] I. Savellii, J.C. Jules, G. Gadret, B. Kibler, J. Fatome, M. El-Amraoui, N. Manikandan, X. Zheng, F. Désévéday, J.M. Dudley, J. Troles, L. Brilland, G. Renversez, F. Smektala, Suspended core tellurite glass optical fibers for infrared supercontinuum generation, *Opt. Mater.* 33 (2011) 1661–1666. doi:10.1016/j.optmat.2011.05.010.
- [7] R. Stegeman, L. Jankovic, H. Kim, C. Rivero, G. Stegeman, K. Richardson, P. Delfyett, Y. Guo, A. Schulte, T. Cardinal, Tellurite glasses with peak absolute Raman gain coefficients up to 30 times that of fused silica, *Opt. Lett.* 28 (2003) 1126–1128. doi:10.1364/OL.28.001126.
- [8] M.D. O'Donnell, K. Richardson, R. Stolen, A.B. Seddon, D. Furniss, V.K. Tikhomirov, C. Rivero, M. Ramme, R. Stegeman, G. Stegeman, M. Couzi, T. Cardinal, Tellurite and fluorotellurite glasses for fiberoptic Raman amplifiers: glass characterization, optical properties, Raman gain, preliminary fiberization, and fiber characterization, *J. Am. Ceram. Soc.* 90 (2007) 1448–1457. doi:10.1111/j.1551-2916.2007.01574.x.
- [9] T. Suzuki, T.W. Shiosaka, S. Miyoshi, Y. Ohishi, Computational and Raman studies of phospho-tellurite glasses as ultrabroad Raman gain media, *J. Non-Cryst. Solids.* 357 (2011) 2702–2707. doi:10.1016/j.jnoncrysol.2011.02.040.
- [10] Z. Shi-An, S. Zhen-Rong, Y. Xi-Hua, W. Zu-Geng, L. Jian, H. Wen-Hai, Femtosecond laser-induced transient grating in CeO₂-doped 75TeO₂–20Nb₂O₅–5ZnO glass, *Chin. Phys.* 14 (2005) 1578–1580. doi:10.1088/1009-1963/14/8/018.
- [11] W. Gao, M. Liao, H. Kawashima, T. Cheng, T. Suzuki, Y. Ohishi, 100-nanosecond-level square-pulse generation in a ring cavity with a tellurite single-mode fiber, *Jpn. J. Appl. Phys.* 51 (2012) 122702. doi:10.1143/JJAP.51.122702.
- [12] S.V. Muravyev, E.A. Anashkina, A.V. Andrianov, V.V. Dorofeev, S.E. Motorin, M.Y. Koptev, A.V. Kim, Dual-band Tm³⁺-doped tellurite fiber amplifier and laser at 1.9 μm and 2.3 μm, *Sci. Rep.* 8 (2018) 16164. doi:10.1038/s41598-018-34546-w.
- [13] B.I. Denker, V.V. Dorofeev, B.I. Galagan, V.V. Koltashev, S.E. Motorin, V.G. Plotnichenko, S.E. Sverchkov, 2.3 μm laser action in Tm³⁺-doped tellurite glass fiber, *Laser Phys. Lett.* 16 (2019) 015101. doi:10.1088/1612-202X/aaeda4.
- [14] E. Fargin, A. Berthereau, T. Cardinal, G. Le Flem, L. Ducasse, L. Canioni, P. Segonds, L. Sarger, A. Ducasse, Optical non-linearity in oxide glasses, *J. Non-Cryst. Solids.* 203 (1996) 96–101. doi:10.1016/0022-3093(96)00338-9.

- [15] B. Jeansannetas, S. Blanchandin, P. Thomas, P. Marchet, J.C. Champarnaud-Mesjard, T. Merle-Méjean, B. Frit, V. Nazabal, E. Fargin, G. Le Flem, M.O. Martin, B. Bousquet, L. Canioni, S. Le Boiteux, P. Segonds, L. Sarger, Glass structure and optical nonlinearities in thallium(I) tellurium(IV) oxide glasses, *J. Solid State Chem.* 146 (1999) 329–335. doi:10.1006/jssc.1999.8355.
- [16] S. Suehara, P. Thomas, A. Mirgorodsky, T. Merle-Méjean, J.C. Champarnaud-Mesjard, T. Aizawa, S. Hishita, S. Todoroki, T. Konishi, S. Inoue, Non-linear optical properties of TeO₂-based glasses: ab initio static finite-field and time-dependent calculations, *J. Non-Cryst. Solids.* 345–346 (2004) 730–733. doi:10.1016/j.jnoncrysol.2004.08.191.
- [17] S. Suehara, P. Thomas, A.P. Mirgorodsky, T. Merle-Méjean, J.C. Champarnaud-Mesjard, T. Aizawa, S. Hishita, S. Todoroki, T. Konishi, S. Inoue, Localized hyperpolarizability approach to the origin of nonlinear optical properties in TeO₂-based materials, *Phys. Rev. B.* 70 (2004). doi:10.1103/PhysRevB.70.205121.
- [18] E.M. Roginskii, V.G. Kuznetsov, M.B. Smirnov, O. Noguera, J.-R. Duclère, M. Colas, O. Masson, P. Thomas, Comparative Analysis of the Electronic Structure and Nonlinear Optical Susceptibility of α -TeO₂ and β -TeO₃ Crystals, *J. Phys. Chem. C.* 121 (2017) 12365–12374. doi:10.1021/acs.jpcc.7b01819.
- [19] A.P. Mirgorodsky, M. Soulis, P. Thomas, T. Merle-Méjean, M. Smirnov, Ab initio study of the nonlinear optical susceptibility of TeO₂-based glasses, *Phys. Rev. B.* 73 (2006) 134206. doi:10.1103/PhysRevB.73.134206.
- [20] M. Soulis, T. Merle-Méjean, A.P. Mirgorodsky, O. Masson, E. Orhan, P. Thomas, M.B. Smirnov, Local molecular orbitals and hyper-susceptibility of TeO₂ glass, *J. Non-Cryst. Solids.* 354 (2008) 199–202. doi:10.1016/j.jnoncrysol.2007.07.036.
- [21] M. Smirnov, A. Mirgorodsky, O. Masson, P. Thomas, Quantum mechanical study of pre-dissociation enhancement of linear and nonlinear polarizabilities of (TeO₂)_n oligomers as a key to understanding the remarkable dielectric properties of TeO₂ glasses, *J. Phys. Chem. A.* 116 (2012) 9361–9369. doi:10.1021/jp303014k.
- [22] N. Berkaine, J. Cornette, D. Hamani, P. Thomas, O. Masson, A. Mirgorodsky, M. Colas, J. Duclère, T. Merle-Méjean, J.-C. Champarnaud-Mesjard, M. Smirnov, Structure and dielectric properties of tellurium oxide-based materials, *Adv. Electroceramic Mater. II.* (2010) 63–74. doi:10.1002/9780470930915.ch7.
- [23] T. Sekiya, N. Mochida, A. Ohtsuka, M. Tonokawa, Raman spectra of MO_{1/2}-TeO₂ (M = Li, Na, K, Rb, Cs and Tl) glasses, *J. Non-Cryst. Solids.* 144 (1992) 128–144. doi:10.1016/S0022-3093(05)80393-X.
- [24] J.C. McLaughlin, S.L. Tagg, J.W. Zwanziger, The structure of alkali tellurite glasses, *J. Phys. Chem. B.* 105 (2001) 67–75. doi:10.1021/jp0025779.
- [25] T. Sekiya, N. Mochida, S. Ogawa, Structural study of WO₃-TeO₂ glasses, *J. Non-Cryst. Solids.* 176 (1994) 105–115. doi:10.1016/0022-3093(94)90067-1.
- [26] I. Shaltout, Y. Tang, R. Braunstein, A.M. Abu-Elazm, Structural studies of tungstate-tellurite glasses by Raman spectroscopy and differential scanning calorimetry, *J. Phys. Chem. Solids.* 56 (1995) 141–150. doi:10.1016/0022-3697(94)00150-2.
- [27] S. Blanchandin, P. Marchet, P. Thomas, J.C. Champarnaud-Mesjard, B. Frit, A. Chagraoui, New investigations within the TeO₂-WO₃ system: phase equilibrium diagram and glass crystallization, *J. Mater. Sci.* 34 (1999) 4285–4292. doi:10.1023/A:1004667223028.
- [28] P. Charton, L. Gengembre, P. Armand, TeO₂-WO₃ glasses: Infrared, XPS and XANES structural characterizations, *J. Solid State Chem.* 168 (2002) 175–183. doi:10.1006/jssc.2002.9707.

- [29] G. Upender, S. Bharadwaj, A.M. Awasthi, V. Chandra Mouli, Glass transition temperature-structural studies of tungstate tellurite glasses, *Mater. Chem. Phys.* 118 (2009) 298–302. doi:10.1016/j.matchemphys.2009.07.058.
- [30] A. Kaur, A. Khanna, V.G. Sathe, F. Gonzalez, B. Ortiz, Optical, thermal, and structural properties of $\text{Nb}_2\text{O}_5\text{-TeO}_2$ and $\text{WO}_3\text{-TeO}_2$ glasses, *Phase Transit.* 86 (2013) 598–619. doi:10.1080/01411594.2012.727998.
- [31] S. Shen, M. Naftaly, A. Jha, Tungsten–tellurite—a host glass for broadband EDFA, *Opt. Commun.* 205 (2002) 101–105. doi:10.1016/S0030-4018(02)01309-3.
- [32] A. Berthereau, Y. Le Luyer, R. Olazcuaga, G. Le Flem, M. Couzi, L. Canioni, P. Segonds, L. Sarger, A. Ducasse, Nonlinear optical properties of some tellurium (IV) oxide glasses, *Mater. Res. Bull.* 29 (1994) 933–941. doi:10.1016/0025-5408(94)90053-1.
- [33] S. Blanchandin, P. Thomas, P. Marchet, J.C. Champarnaud-Mesjard, B. Frit, Equilibrium and non-equilibrium phase diagram within the TeO_2 -rich part of the $\text{TeO}_2\text{-Nb}_2\text{O}_5$ system, *J. Mater. Chem.* 9 (1999) 1785–1788. doi:10.1039/a900788a.
- [34] M. Soulis, Structure et propriétés optiques non linéaires des verres à base d'oxyde de tellure : approche cristalochimique et calculs ab-initio, PhD thesis, Université de Limoges, 2007.
- [35] M.A. Villegas, J.M.F. Navarro, Physical and structural properties of glasses in the $\text{TeO}_2\text{-TiO}_2\text{-Nb}_2\text{O}_5$ system, *J. Eur. Ceram. Soc.* 27 (2007) 2715–2723. doi:10.1016/j.jeurceramsoc.2006.12.003.
- [36] J. Lin, W. Huang, L. Ma, Q. Bian, S. Qin, H. Wei, J. Chen, Crystallization of $\text{TeO}_2\text{-Nb}_2\text{O}_5$ glasses and their network structural evolution, *Materials Science-Poland.* 27 (2009).
- [37] T. Hayakawa, M. Hayakawa, M. Nogami, P. Thomas, Nonlinear optical properties and glass structure for $\text{MO-Nb}_2\text{O}_5\text{-TeO}_2$ (M=Zn, Mg, Ca, Sr, Ba) glasses, *Opt. Mater.* 32 (2010) 448–455. doi:10.1016/j.optmat.2009.10.006.
- [38] G. Senthil Murugan, Y. Ohishi, $\text{TeO}_2\text{-BaO-SrO-Nb}_2\text{O}_5$ glasses: a new glass system for waveguide devices applications, *J. Non-Cryst. Solids.* 341 (2004) 86–92. doi:10.1016/j.jnoncrysol.2004.04.006.
- [39] S. Dai, J. Wu, J. Zhang, G. Wang, Z. Jiang, The spectroscopic properties of Er^{3+} -doped $\text{TeO}_2\text{-Nb}_2\text{O}_5$ glasses with high mechanical strength performance, *Spectrochim. Acta. A. Mol. Biomol. Spectrosc.* 62 (2005) 431–437. doi:10.1016/j.saa.2005.01.011.
- [40] U. Hoppe, E. Yousef, C. Rüssel, J. Neuefeind, A.C. Hannon, Structure of zinc and niobium tellurite glasses by neutron and x-ray diffraction, *J. Phys. Condens. Matter.* 16 (2004) 1645–1663. doi:10.1088/0953-8984/16/9/013.
- [41] A. Berthereau, E. Fargin, A. Villezusanne, R. Olazcuaga, G. Le Flem, L. Ducasse, Determination of local geometries around tellurium in $\text{TeO}_2\text{-Nb}_2\text{O}_5$ and $\text{TeO}_2\text{-Al}_2\text{O}_3$ oxide glasses by XANES and EXAFS: Investigation of electronic properties of evidenced oxygen clusters by ab initio calculations, *J. Solid State Chem.* 126 (1996) 143–151. doi:10.1006/jssc.1996.0322.
- [42] Y.B. Saddeek, E.R. Shaaban, F.M. Abdel-Rahim, K.H. Mahmoud, Thermal analysis and infrared study of $\text{Nb}_2\text{O}_5\text{-TeO}_2$ glasses, *Philos. Mag.* 88 (2008) 3059–3073. doi:10.1080/14786430802499012.
- [43] M.R. Zaki, D. Hamani, M. Dutreilh-Colas, J.-R. Duclère, O. Masson, P. Thomas, Synthesis, thermal, structural and linear optical properties of new glasses within the $\text{TeO}_2\text{-TiO}_2\text{-WO}_3$ system, *J. Non-Cryst. Solids.* 484 (2018) 139–148. doi:10.1016/j.jnoncrysol.2018.01.034.
- [44] J. Carreaud, A. Labruyère, H. Dardar, F. Moisy, J.-R. Duclère, V. Couderc, A. Bertrand, M. Dutreilh-Colas, G. Delaizir, T. Hayakawa, A. Crunteanu, P. Thomas, Lasing effects

- in new Nd³⁺-doped TeO₂-Nb₂O₅-WO₃ bulk glasses, *Opt. Mater.* 47 (2015) 99–107. doi:10.1016/j.optmat.2015.06.055.
- [45] G. Dai, F. Tassone, A. LiBassi, V. Russo, C.E. Bottani, F. D'Amore, TeO₂-based glasses containing Nb₂O₅, TiO₂, and WO₃ for discrete Raman fiber amplification, *IEEE Photonics Technol. Lett.* 16 (2004) 1011–1013. doi:10.1109/LPT.2004.824963.
- [46] D.M. Munoz-Martín, TeO₂-based film glasses for photonic applications: structural and optical properties., PhD, Universidad Complutense de Madrid, 2010.
- [47] S. Xu, S. Dai, J. Zhang, L. Hu, Z. Jiang, Broadband 1.5- μ m emission of erbium-doped TeO₂-WO₃-Nb₂O₅ glass for potential WDM amplifier, *Chin. Opt. Lett.* 2 (2004) 106–108.
- [48] X. Wang, Investigation of thermal stability and spectroscopic properties in Er³⁺/Yb³⁺ co-doped niobic tungsten tellurite glasses, *Spectrochim. Acta. A. Mol. Biomol. Spectrosc.* 70 (2008) 99–103. doi:10.1016/j.saa.2007.07.013.
- [49] D. De Sousa Meneses, Software utility for the creation of optical function (FOCUS), CEMHTI UPR 3079 CNRS Orléans, France, 2004. <http://www.cemhti.cnrs-orleans.fr/pot/software/focus.html>.
- [50] J.-R. Duclère, T. Hayakawa, E.M. Roginskii, M.B. Smirnov, A. Mirgorodsky, V. Couderc, O. Masson, M. Colas, O. Noguera, V. Rodriguez, P. Thomas, Third order nonlinear optical properties of a paratellurite single crystal, Accepted for publication in *J. Appl. Phys.*, 123 (2018).
- [51] M. Sheik-Bahae, A.A. Said, T.-H. Wei, D.J. Hagan, E.W. Van Stryland, Sensitive measurement of optical nonlinearities using a single beam, *IEEE J. Quantum Electron.* 26 (1990) 760–769. doi:10.1109/3.53394.
- [52] D. Milam, Review and assessment of measured values of the nonlinear refractive-index coefficient of fused silica, *Appl. Opt.* 37 (1998) 546. doi:10.1364/AO.37.000546.
- [53] S.-H. Kim, T. Yoko, S. Sakka, Linear and nonlinear optical properties of TeO₂ glass, *J. Am. Ceram. Soc.* 76 (1993) 2486–2490. doi:10.1111/j.1151-2916.1993.tb03970.x.
- [54] D. Linda, J.-R. Duclère, T. Hayakawa, M. Dutreilh-Colas, T. Cardinal, A. Mirgorodsky, A. Kabadou, P. Thomas, Optical properties of tellurite glasses elaborated within the TeO₂-Tl₂O-Ag₂O and TeO₂-ZnO-Ag₂O ternary systems, *J. Alloys Compd.* 561 (2013) 151–160. doi:10.1016/j.jallcom.2013.01.172.
- [55] M. Sundberg, The crystal and defect structures of W₂₅O₇₃, a member of the homologous series W_nO_{3n-2}, *Acta Crystallogr. B.* 32 (1976) 2144–2149. doi:10.1107/S0567740876007280.
- [56] I.A. Khodyakova, V.A. Dolgikh, B.A. Popovkin, A.V. Novoselova, *Russ. J. Inorg. Chem.* 27 (1982) 1235–1241.
- [57] Y.-R. Luo, *Comprehensive handbook of chemical bond energies*, CRC Press, Boca Raton, 2007.
- [58] A.P. Mirgorodsky, T. Merle-Méjean, J.-C. Champarnaud, P. Thomas, B. Frit, Dynamics and structure of TeO₂ polymorphs: model treatment of paratellurite and tellurite; Raman scattering evidence for new γ - and δ -phases, *J. Phys. Chem. Solids.* 61 (2000) 501–509. doi:10.1016/S0022-3697(99)00263-2.
- [59] J.C. Champarnaud-Mesjard, S. Blanchandin, P. Thomas, A. Mirgorodsky, T. Merle-Méjean, B. Frit, Crystal structure, Raman spectrum and lattice dynamics of a new metastable form of tellurium dioxide: γ -TeO₂, *J. Phys. Chem. Solids.* 61 (2000) 1499–1507. doi:10.1016/S0022-3697(00)00012-3.
- [60] A.P. Sokolov, A. Kisliuk, M. Soltwisch, D. Quitmann, Medium-range order in glasses: Comparison of Raman and diffraction measurements, *Phys. Rev. Lett.* 69 (1992) 1540–1543. doi:10.1103/PhysRevLett.69.1540.

- [61] T. Vasileiadis, S.N. Yannopoulos, Photo-induced oxidation and amorphization of trigonal tellurium: A means to engineer hybrid nanostructures and explore glass structure under spatial confinement, *J. Appl. Phys.* 116 (2014) 103510. doi:10.1063/1.4894868.
- [62] M.F. Daniel, B. Desbat, J.C. Lassegues, B. Gerand, M. Figlarz, Infrared and Raman study of WO_3 tungsten trioxides and $\text{WO}_3 \cdot x\text{H}_2\text{O}$ tungsten trioxide hydrates, *J. Solid State Chem.* 67 (1987) 235–247. doi:10.1016/0022-4596(87)90359-8.
- [63] O. Noguera, T. Merle-Méjean, A.P. Mirgorodsky, P. Thomas, J.-C. Champarnaud-Mesjard, Dynamics and crystal chemistry of tellurites. II. Composition- and temperature-dependence of the Raman spectra of $x(\text{Ti}_2\text{O})+(1-x)\text{TeO}_2$ glasses: evidence for a phase separation?, *J. Phys. Chem. Solids.* 65 (2004) 981–993. doi:10.1016/j.jpcs.2003.11.020.
- [64] N. Ghribi, Synthèse, caractérisations structurale et élastique de nouveaux matériaux tellurites pour des applications en optique non linéaire, PhD thesis, Université de Limoges, 2015.
- [65] G. Upender, C.P. Vardhani, S. Suresh, A.M. Awasthi, V. Chandra Mouli, Structure, physical and thermal properties of $\text{WO}_3\text{--GeO}_2\text{--TeO}_2$ glasses, *Mater. Chem. Phys.* 121 (2010) 335–341. doi:10.1016/j.matchemphys.2010.01.050.
- [66] A.G. Kalampounias, G.N. Papatheodorou, S.N. Yannopoulos, A temperature dependence Raman study of the $0.1 \text{ Nb}_2\text{O}_5\text{--}0.9 \text{ TeO}_2$ glass-forming system, *J. Phys. Chem. Solids.* 67 (2006) 725–731. doi:10.1016/j.jpcs.2005.11.001.
- [67] A.M. Efimov, V.G. Pogareva, A.V. Shashkin, Water-related bands in the IR absorption spectra of silicate glasses, *J. Non-Cryst. Solids.* 332 (2003) 93–114. doi:10.1016/j.jnoncrysol.2003.09.020.
- [68] E.S. Yousef, A. El-Adawy, N. El Koshkhany, E.R. Shaaban, Optical and acoustic properties of $\text{TeO}_2\text{--WO}_3$ glasses with small amount of additive ZrO_2 , *J. Phys. Chem. Solids.* 67 (2006) 1649–1655. doi:10.1016/j.jpcs.2006.02.014.
- [69] M.M. Umair, A.K. Yahya, M.K. Halimah, H.A.A. Sidek, Effects of increasing tungsten on structural, elastic and optical properties of $x\text{WO}_3\text{--}(40-x)\text{Ag}_2\text{O--}60\text{TeO}_2$ Glass System, *J. Mater. Sci. Technol.* 31 (2015) 83–90. doi:10.1016/j.jmst.2014.10.002.
- [70] F. Urbach, The long-wavelength edge of photographic sensitivity and of the electronic absorption of solids, *Phys. Rev.* 92 (1953) 1324–1324. doi:10.1103/PhysRev.92.1324.
- [71] Sellmeier, Zur Erklärung der abnormen Farbenfolge im Spectrum einiger Substanzen, *Ann. Phys. Chem.* 219 (1871) 272–282. doi:10.1002/andp.18712190612.
- [72] G. Ghosh, Sellmeier coefficients and dispersion of thermo-optic coefficients for some optical glasses, *Appl. Opt.* 36 (1997) 1540. doi:10.1364/AO.36.001540.
- [73] M.E. Lines, Influence of d orbitals on the nonlinear optical response of transparent transition-metal oxides, *Phys. Rev. B.* 43 (1991) 11978–11990. doi:10.1103/PhysRevB.43.11978.